

**Predicting the Effects of Process Parameters on Weldment
Characteristics in MIG Welding using
Artificial Neural Networks**



by

SUBRATA SAHA

A project submitted in partial fulfillment of the requirements for the degree of
Master of Science in Engineering in Mechanical Engineering Department



Khulna University of Engineering and Technology

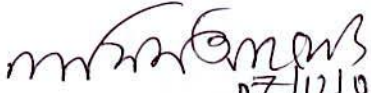
Khulna – 9203, Bangladesh


December, 2009

Declaration

This is to certify that the project work entitled *Predicting the Effects of Process Parameters on Weldment Characteristics in MIG Welding using Artificial Neural Networks* has been carried out by *Subrata Saha* in the Department of Mechanical Engineering, Khulna University of Engineering & Technology, Khulna, Bangladesh. The above research work or any part of the work has not been submitted anywhere for the award of any degree or diploma.




07/12/09
(Dr. Naseem Ahmed)
Professor
Department of Mechanical Engineering


07/12/09
(Subrata Saha)
Roll No - 0405502



Approval

This is to certify that the project work submitted by *Subrata Saha* entitled *Predicting the Effects of Process Parameters on Weldment Characteristics in MIG Welding using Artificial Neural Networks* has been approved by the Board of Examiners for the partial fulfillment of the requirements for the degree of *Master of Science in Engineering* in the Department of *Mechanical Engineering*, Khulna University of Engineering & Technology, Khulna, Bangladesh in *December, 2009*.

BOARD OF EXAMINERS

1. Dr. Naseem Ahmed
Professor
Department of Mechanical Engineering
Khulna University of Engineering & Technology
2. Dr. Tarapada Bhowmick
Professor & Head
Department of Mechanical Engineering
Khulna University of Engineering & Technology
3. Dr. Khandkar Aftab Hossain
Professor
Department of Mechanical Engineering
Khulna University of Engineering & Technology
4. Dr. Md. Syed Ali Mollah
Professor
Department of Mechanical Engineering
Khulna University of Engineering & Technology
5. Dr. Md. Shamim Akhter
Professor
Department of Mechanical Engineering
Rajshahi University of Engineering & Technology

Chairman
(Supervisor)

Member
Member 30.12.09
Member 30/12/2009
Member
(External)

Acknowledgement

The author would like to express sincere gratitude and profound indebtedness to the respectful teacher Dr. Naseem Ahmed, Professor, Department of Mechanical Engineering, Khulna University of Engineering & Technology, Khulna, Bangladesh for his kind supervision, guidance, advice, help and also encouragement to complete the research work as well as in preparing this project report.

The author would like to express gratefulness to the all senior teachers including Professor Dr. Tarapada Bhowmick, Head of the Department, Department of Mechanical Engineering, Khulna University of Engineering & Technology, Khulna for their inspiration and encouragement to complete the project work in due time. Author is thankful to Dr. Md. Abdur Rafiq, Associate Professor, Department of Electrical and Electronic Engineering, Khulna University of Engineering & Technology, Khulna for his kind help and co-operation to complete the computational task including computer programming with artificial neural network model.

Thanks to the executive of *Hope Technical Institute (HTI)*, a sister concern of CSS, Sonadanga, Khulna and *Bangladesh Industry and Technical Assistance Centre (BITAC)*, Siromoni, Khulna for extending their kind help to perform various part of experimental works.

The author is grateful to all staff member of Machine shop, Welding shop, Metallurgy Laboratory of the Department of Mechanical Engineering of Khulna University of Engineering & Technology, Khulna for their cordial help to perform different experimental works. Especially thanks are due to Mr. Md. Rafiqul Islam, ATO for his cordial behavior and providing full extent of help.

Lastly, the author expresses his heartfelt gratitude to his father, mother and other beloved family members for their blessings and moral supports.

Khulna

Subrata Saha
Author

Abstract

In this project work an attempt has been taken to predicting the effects of process parameters on weldment characteristics in MIG welding with the help of artificial neural network technique.

Electrode wire diameter, Electrode wire feed rate, Welding speed, Welding current and Arc length have been chosen as influential process parameters. More or less, these are the influential factors in deciding the weldment characteristics.

Weldment characteristics like Bead Geometry, Depth of Penetration, Depth of Heat Affected Zone (HAZ) and Hardness of weld metal are important characteristics on the basis of structure and these have been considered in this project work.

Metal Inert Gas (MIG) Welding process with automatic or robotic system in various industries is a demanding welding process now-a-days and this process is being used with increasing rate of applications. Due to these reasons, MIG welding process has been chosen for this project work and a semi-automatic MIG welding machine have been used. Single straight beads have been welded on the surface of the specimens of the medium carbon steel plate.

Artificial Neural Network (ANN) refers to computing systems whose central theme is borrowed from the analogy of biological neural networks and the basic unit of such networks is a simple mathematical model. In this research work the Real-Time Recurrent Learning algorithm of ANN have been used with actual inputs and outputs of experimental values as inputs to the algorithm to complete the computational tasks.

It has been observed that the computational values of weldment characteristics obtained by ANN are very close to the experimental values of those. So the ANN based approach can be used effectively for predicting the weldment characteristics in MIG welding.

Contents

	PAGE
Title page	i
Declaration	ii
Approval	iii
Acknowledgement	iv
Abstract	v
Contents	vi
List of Tables	vii
List of Figures	viii
CHAPTER 1	
Introduction	1
1.1 General Introduction	1
1.2 Welding Basics and MIG Welding	3
CHAPTER 2	
Literature Review	12
2.1 Research Works	12
CHAPTER 3	
Artificial Neural Network	18
3.1 Introduction	18
3.2 Models of a Neuron	20
3.3 Activation Function	23
3.4 Network Architectures	26
3.5 Neural Learning	30
CHAPTER 4	
Procedures / Methodology	39
4.1 Introduction	39
4.2 Experimental Procedures	40
CHAPTER 5	
Results and Discussions	46
5.1 Results	46
5.2 Discussions	61
CHAPTER 6	
Conclusions and Recommendations	65
6.1 Conclusions	65
6.2 Recommendations	67
REFERENCES	68
APPENDICES	70 – 90



List of Tables

Table No	Caption of the Table	Page
3.5	Summary of the Real-Time Recurrent Learning Algorithm	37
5.1 (a)	Experimental values of Bead Width, Bead Height, Depth of Penetration & Heat Affected Zone and Hardness using current range from 194 – 263 amp for electrode wire diameter and feed rate respectively 0.8 mm and 4600 mm/min.	47
5.1 (b)	Experimental values of Bead Width, Bead Height, Depth of Penetration & Heat Affected Zone and Hardness using current range from 271 – 340 amp for electrode wire diameter and feed rate respectively 0.8 mm and 5600 mm/min.	47
5.1 (c)	Experimental values of Bead Width, Bead Height, Depth of Penetration & Heat Affected Zone and Hardness using current range from 194 – 263 amp for electrode wire diameter and feed rate respectively 1.0 mm and 4600 mm/min.	48
5.1 (d)	Experimental values of Bead Width, Bead Height, Depth of Penetration & Heat Affected Zone and Hardness using current range from 271 – 340 amp for electrode wire diameter and feed rate respectively 1.0 mm and 5600 mm/min.	48
5.1 (e)	Computational values of Bead Width, Bead Height, Depth of Penetration & Heat Affected Zone and Hardness using current range from 194 – 263 amp for electrode wire diameter and feed rate respectively 0.8 mm and 4600 mm/min.	49
5.1 (f)	Computational values of Bead Width, Bead Height, Depth of Penetration & Heat Affected Zone and Hardness using current range from 271 – 340 amp for electrode wire diameter and feed rate respectively 0.8 mm and 5600 mm/min.	49
5.1 (g)	Computational values of Bead Width, Bead Height, Depth of Penetration & Heat Affected Zone and Hardness using current range from 194 – 263 amp for electrode wire diameter and feed rate respectively 1.0 mm and 4600 mm/min.	50
5.1 (h)	Computational values of Bead Width, Bead Height, Depth of Penetration & Heat Affected Zone and Hardness using current range from 271 – 340 amp for electrode wire diameter and feed rate respectively 1.0 mm and 5600 mm/min.	50

List of Figures

Figure No	Caption of the Figure	Page
1.2 (a)	Photograph of MIG Welding Machine, Equipments and Welder	8
1.2 (b)	MIG Welding Setup	9
1.2 (c)	MIG Welding Operation	9
3.2 (a)	Nonlinear Model of a Neuron	20
3.2 (b)	Affine Transformation produced by the presence of a bias; note that $v_k = b_k$ at $u_k = 0$	21
3.2 (c)	Another Nonlinear Model of a Neuron	22
3.3 (a)	Threshold Function	23
3.3 (b)	Piecewise-Linear Function	24
3.3 (c)	Sigmoid Function for varying slope parameter 'a'	25
3.4 (a)	Feed forward or Acyclic Network with a Single Layer of Neurons	26
3.4 (b)	Fully Connected Feed forward or Acyclic Network with One Hidden Layer and One Output Layer	28
3.4 (c)	Recurrent Network with no Self-Feedback Loops and no Hidden Neurons	28
3.4 (d)	Recurrent Network with Hidden Neurons	29
3.5 (a)	Block Diagram of A Learning with a Teacher	32
3.5 (b)	Fully connected recurrent network for formulation of the RTRL algorithm	34
4.2 (a)	Sketch of specimen with dimensional configuration	40
4.2 (b)	Photograph of MIG welding operation	43
4.2 (c)	Photograph of Weldment	43
4.2 (d)	Sketch of Weld Bead Geometry and Heat Affected Zone	44
4.2 (e)	Photograph of Bead Width, Bead Height, Penetrated and Heat Affected Zone of weldment	44
5.1 (a)	Comparison of Bead Width values using current range from 194 - 263 amp, electrode wire diameter and feed rate respectively 0.8 mm and 4600 mm/min.	51
5.1 (b)	Comparison of Bead Width values using current range from 271 - 340 amp, electrode wire diameter and feed rate respectively 0.8 mm and 5600 mm/min.	51
5.1 (c)	Comparison of Bead Width values using current range from 194 - 263 amp, electrode wire diameter and feed rate respectively 1.0 mm and 4600 mm/min.	52
5.1 (d)	Comparison of Bead Width values using current range from 271 - 340 amp, electrode wire diameter and feed rate respectively 1.0 mm and 5600 mm/min.	52
5.1 (e)	Comparison of Bead Height values using current range from 194 - 263 amp, electrode wire diameter and feed rate respectively 0.8 mm and 4600 mm/min.	53
5.1 (f)	Comparison of Bead Height values using current range from 271 - 340 amp, electrode wire diameter and feed rate respectively 0.8 mm and 5600 mm/min.	53

Figure No	Caption of the Figure	Page
5.1 (g)	Comparison of Bead Height values using current range from 194 - 263 amp, electrode wire diameter and feed rate respectively 1.0 mm and 4600 mm/min.	54
5.1 (h)	Comparison of Bead Height values using current range from 271 - 340 amp, electrode wire diameter and feed rate respectively 1.0 mm and 5600 mm/min.	54
5.1 (i)	Comparison of Depth of Penetration values using current range from 194 - 263 amp, electrode wire diameter and feed rate respectively 0.8 mm and 4600 mm/min.	55
5.1 (j)	Comparison of Depth of Penetration values using current range from 271 - 340 amp, electrode wire diameter and feed rate respectively 0.8 mm and 5600 mm/min.	55
5.1 (k)	Comparison of Depth of Penetration values using current range from 194 - 263 amp, electrode wire diameter and feed rate respectively 1.0 mm and 4600 mm/min.	56
5.1 (l)	Comparison of Depth of Penetration values using current range from 271 - 340 amp, electrode wire diameter and feed rate respectively 1.0 mm and 5600 mm/min.	56
5.1 (m)	Comparison of Depth of HAZ values using current range from 194 - 263 amp, electrode wire diameter and feed rate respectively 0.8 mm and 4600 mm/min.	57
5.1 (n)	Comparison of Depth of HAZ values using current range from 271 - 340 amp, electrode wire diameter and feed rate respectively 0.8 mm and 5600 mm/min.	57
5.1 (o)	Comparison of Depth of HAZ values using current range from 194 - 263 amp, electrode wire diameter and feed rate respectively 1.0 mm and 4600 mm/min.	58
5.1 (p)	Comparison of Depth of HAZ values using current range from 271 - 340 amp, electrode wire diameter and feed rate respectively 1.0 mm and 5600 mm/min.	58
5.1 (q)	Comparison of Hardness values using current range from 194 - 263 amp, electrode wire diameter and feed rate respectively 0.8 mm and 4600 mm/min.	59
5.1 (r)	Comparison of Hardness values using current range from 271 - 340 amp, electrode wire diameter and feed rate respectively 0.8 mm and 5600 mm/min.	59
5.1 (s)	Comparison of Hardness values using current range from 194 - 263 amp, electrode wire diameter and feed rate respectively 1.0 mm and 4600 mm/min.	60
5.1 (t)	Comparison of Hardness values using current range from 271 - 340 amp, electrode wire diameter and feed rate respectively 1.0 mm and 5600 mm/min.	60

CHAPTER 1

INTRODUCTION



1.1 General Introduction

On the basis of industrial fabrication application, due to various reasons welding is a very versatile and useful process. In most cases time, labor, cost and structural integrity are effective with respect to different types of welding method, applicable welding conditions, process implementation method, base material and size etc. Now-a-days some welding methods are useful in industry around the world on the basis of above reasons satisfactorily. MIG welding process is one of them whose demand is increasing rapidly but eventually a little research work has been done with that. So, MIG welding process has been chosen for this work.

Actually there has a lot of scope to work in MIG welding process due to different process parameters and weldment characteristics to consider. But due to the limitations of the availability of experimental facilities; in this research work the process parameters and weldment characteristics have been considered to some limited numbers.

Predicting is nothing but in simple sense is understanding about what will happen and how much intensive that will be on outputs of a process by varying inputs. Incase of this research work inputs are some process parameters of MIG welding process and outputs are weldment characteristics. Predicting processes are of different types; among them - Mathematical modeling, Numerical analysis and Artificial Neural Network modeling are most acceptable and reasonable due to various reasons. As mentioned in the above Artificial Neural Network modeling has been chosen for this work due to its capability to solve difficult and complex problems and recently welding related many researchers have been using ANN model to understand and predict their targeted information.

In this research work prediction has been done in this way that, by varying some process parameters, e.g., electrode wire diameter, electrode wire feed rate, welding current, etc. consider the variation of weldment characteristics. To do this, Real-Time Recurrent Learning Algorithm, i.e., a supervised learning algorithm of ANN model has been used.

As mentioned in various literatures it is very clear that, with different welding conditions the resulting characteristics of weldment differ significantly. So the main objective of this project work is to predict the weldment characteristics with variations of different MIG welding process parameters. And the other significant goals are as follows:

- To incorporate the modern and versatile MIG welding process; by doing this the experimental task have been performed
- To develop an Artificial Neural Network model and process (train) it using experimental values
- To compare the experimental values with computational (using ANN model) values of weldment characteristics obtained at different process parameters for predicting.

At present there exists a great demand to predict a predetermined quality weldment using MIG with automatic or robotic system in various industries. Not only this, the demand is increasing day by day. So prediction of the effect of process parameters on weldment characteristics is very important and has got a great extent of applications.

1.2 Welding Basics and MIG Welding

1.2.1 Welding Basics

1.2.1.1 Introduction

Welding is a process for joining different materials. The large bulk of materials that are welded are metals and their alloys, although the term welding is also applied to the joining of other materials such as thermoplastics.

Welding joins different metals/alloys with the help of a number of processes in which heat is supplied either electrically or by means of a gas torch. In order to join two or more pieces of metal together by one of the welding processes, the most essential requirement is *Heat*. *Pressure* may also be employed, but this is not, in many processes essential.

The use of welding in today's technology is extensive. It had a phenomenal rise since about 1930; this growth has been faster than the general industrial growth. Many common everyday-use items, e.g., automobile cars, aircrafts, ships, electronic equipment, machinery, household appliances, etc., depend upon welding for their economical construction [1].

1.2.1.2 History of Arc Welding

Electric arc was first described by Davy in England, in the year 1809, but the beginning of arc welding could become possible only with the improvements in electric dynamos or generators between 1877 and 1880. Auguste de Meritens established arc welding process in 1881 which was applied to join certain components of electrical storage batteries.

Arc and molten pool shielding with an inert gas (CO_2) was advertised by Alexander in USA in the year 1928 and the patent for TIG welding was received by Hobart and Devers in 1930 in USA. First gas tungsten arc spot welding torch based upon TIG welding was introduced around 1946. Metal Inert Gas (MIG) welding came out in 1948 as a result of

further researches and developments carried out on Covered Electrode Metal Arc and Tungsten Inert Gas welding processes. The credit for submerged arc welding goes to Kennedy, Rodermund and Jones (1935) of USA. Electro slag welding is a further development of submerged arc welding and it came to appearance round about 1953 in Russia.

Stud welding was found by Martin in 1918 and was used in British (Royal) Navy. Round about 1938, Nelsen rediscovered this process in USA and in about 1958 Van den Blink and others suggested the use of fusible collar in stud welding.

The atomic hydrogen welding was developed on the basis of the research carried out by Langmuir (1921, USA) on the dissociation of diatomic molecule in electric arc. Plasma arc welding is a step ahead of TIG welding. It was developed in USA in the year 1953. Plasma cutting was used in 1955 and satisfactory plasma spraying and plasma welding were carried out in 1960 and 1963 respectively [1].

1.2.1.3 Classification of Welding Processes

There are about 35 different welding and brazing processes and several soldering methods in use by industry today. There are various ways of classifying the welding and allied processes. For example, they may be classified on the basis of:

- Source of heat, i.e., flame, arc, etc.
- Type of interaction, i.e., liquid/liquid (fusion welding) or solid/solid (solid state welding).

In general, various welding and allied processes are classified as follows:

a) Gas Welding

- Air-acetylene Welding
- Oxy-acetylene Welding
- Oxy-hydrogen Welding
- Pressure gas Welding

b) Arc Welding

- Carbon Arc Welding
- Shielded Metal Arc Welding

- Flux Cored Arc Welding
- TIG (or GTAW) Welding
- Plasma Arc Welding
- Submerged Arc Welding
- MIG (or GMAW) Welding
- Electro slag and Electro gas Welding
- Stud Arc Welding
- c) Resistance Welding
 - Spot Welding
 - Projection Welding
 - Flash Butt Welding
 - Seam Welding
 - Resistance Butt Welding
 - Percussion Welding
 - High Frequency Resistance Welding
- d) Solid State Welding
 - Cold Welding
 - Explosive welding
 - Friction Welding
 - Roll Welding
 - Diffusion Welding
 - Forge Welding
 - Hot Pressure Welding
 - Ultrasonic welding
- e) Thermo-Chemical Welding Processes
 - Thermit Welding
 - Atomic Hydrogen Welding
- f) Radiant Energy Welding Processes
 - Electron Beam Welding
 - Laser Beam Welding [1].

1.2.1.4 Commonly Weld able Metals

Metals can be classified as -

a) Ferrous & b) Non-ferrous

a) Ferrous materials contain iron and the one element people use more than all others is iron. Ferrous materials are the most important metals/alloys in the metallurgical and mechanical industries because of their very extensive use. Ferrous materials finding day-to-day welding applications are:

- Wrought Iron
- Carbon Steels (Low, Medium & High Carbon Steels)
- Alloy Steels
- Cast Iron
- Cast Steels
- Stainless Steels , etc.

b) Non-ferrous materials are those that are not iron-based. Like ferrous materials, non-ferrous materials also find extensive industrial applications. Non-ferrous materials finding day-to-day welding applications are:

- Aluminum and its alloys
- Copper and its alloys
- Magnesium and its alloys
- Nickel and its alloys
- Zinc and its alloys, etc. [1].

1.2.1.5 Advantages of Welding

- i) A good weld is as strong as the base metal
- ii) General welding equipment is not very costly and they are portable also
- iii) Welding permits considerable freedom in design
- iv) A large number of metals/alloys both similar and dissimilar can be joined by welding [1].

1.2.1.6 Disadvantages of Welding

- i) Welding gives out harmful radiations (light), fumes and spatter
- ii) Edge preparation of the work pieces is generally required before welding them
- iii) A skilled welder is a must to produce a good welding job
- iv) Welding heat produces metallurgical changes. The structure of the welded joint is not same as that of the parent metal [1].

1.2.1.7 Practical Applications of Welding

Welding has been employed in industry as a tool for:

- a) Regular fabrication of automobile cars, air-crafts, refrigerators, etc.
- b) Repair and maintenance work, e. g., joining broken parts, rebuilding worn out components, etc. [1].

1.2.1.8 A few important applications of welding are listed below:

- Aircraft Construction
 - Buildings
 - Storage Tanks
 - Piping and Pipelines
 - Trucks and Trailers
 - Household and Office Furniture
 - Bridges
 - Pressure Vessels and Tanks
 - Rail Road Equipment
 - Ships
 - Machine tool frames, Cutting tools & Dies
 - Automobile Construction
- Earth moving machinery and Cranes, etc. [1].

1.2.2 Metal Inert Gas (MIG) Welding

1.2.2.1 Definition

It is an arc welding process wherein coalescence is produced by heating the job with an electric arc established between a continuously fed metal electrode and the job. No flux is used but the arc and molten metal are shielded by an inert gas, which may be argon, helium, carbon dioxide or a gas mixture [1].

1.2.2.2 Equipments

- a) Welding power source and cables
- b) Welding torch and wire electrode coiled on a spool
- c) Wire feed mechanism and controls consisting of a pair of driving rolls, electric motor, etc.
- d) Shielding gas cylinder, pressure regulator and flow meter
- e) Controls for switching on and off the current, electrode wire and inert gas [1].



1.2.2.3 Principle of Operation (Semi-automatic process)

Before igniting the arc, gas and water flow is checked. Proper current and wire feed speed is set and the electrical connections are ensured. The arc is struck by any one of the two methods. In the *first method* current and shielding gas flow is switched on and the electrode is scratched against the job as usual practice for striking the arc.

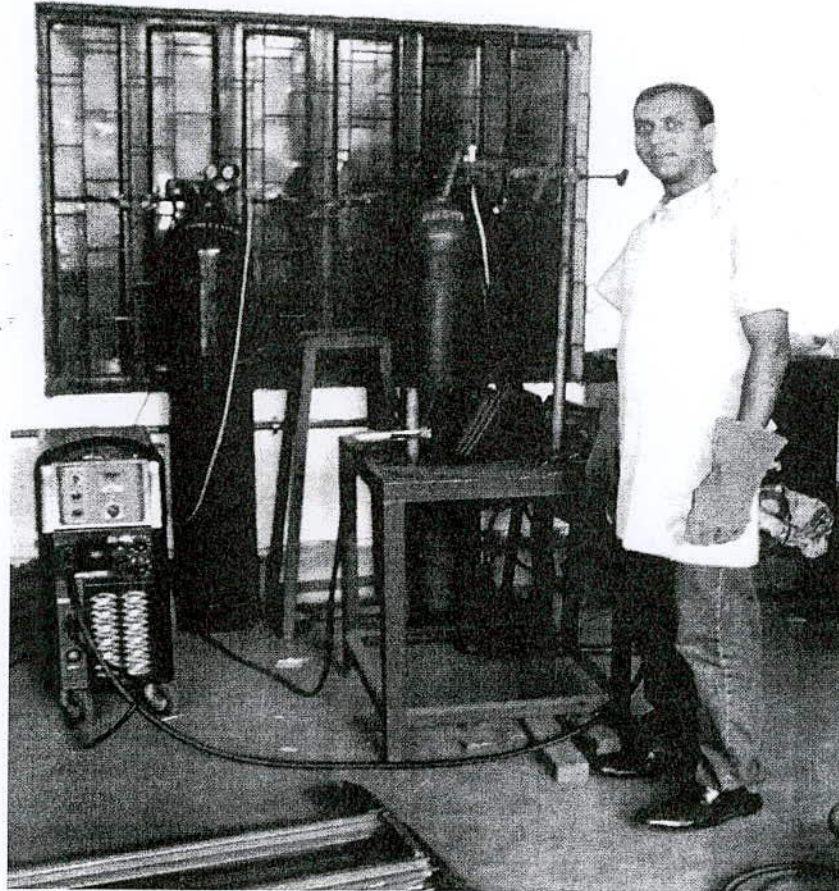


Figure: 1.2 (a) Photograph of MIG Welding Machine, Equipments and Welder

In the *second method*, electrode is made to touch the job, is retracted and then moved forward to carry out welding; but before striking the arc, shielding gas, water and current is switched on. About 15 mm length of the electrode is projected from the torch before striking the arc. During welding, torch remains about 10-12 mm away from the job and arc length is kept between 1.5 to 4 mm.

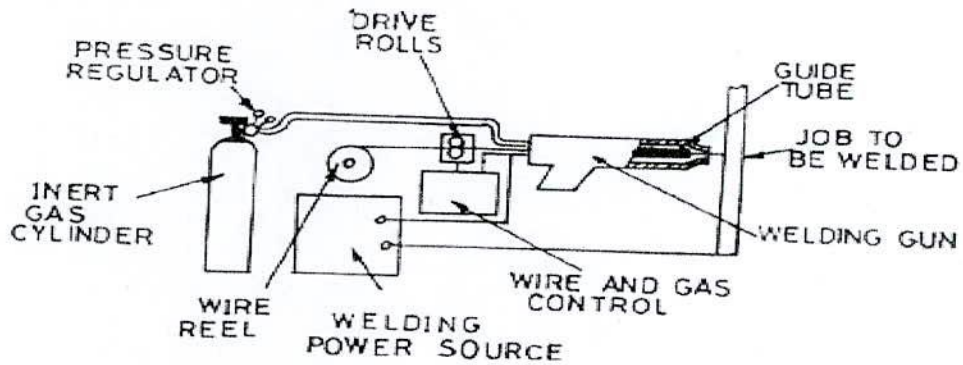


Figure: 1.2 (b) MIG Welding Setup

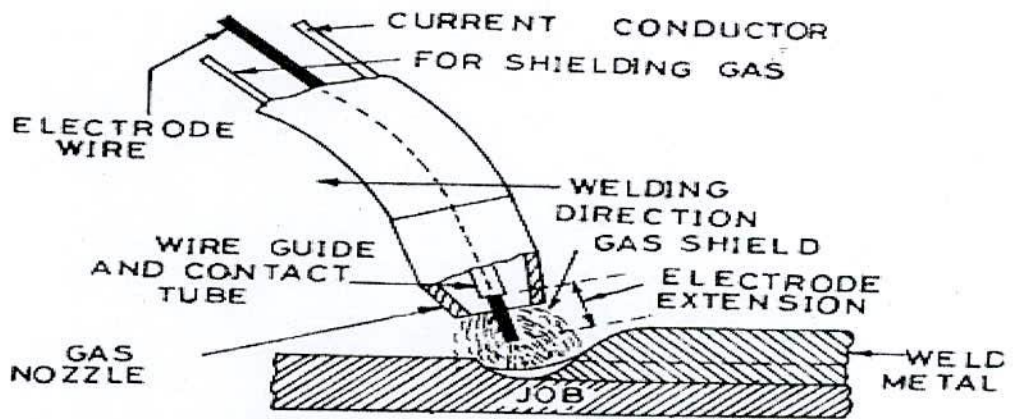


Figure: 1.2 (c) MIG Welding Operation

Arc length is maintained constant by using the principles of self-adjusted arc, and self-controlled arc in semi-automatic (manually operated) and automatic welding sets respectively [1].

1.2.2.4 Metals Welded

Base metals commonly welded by MIG Welding are:

- i) Carbon and low alloy steels
- ii) Stainless steels
- iii) Heat-resisting alloys

- iv) Aluminum and its alloys
- v) Copper and its alloys (other than high zinc alloys)
- vi) Magnesium alloys [1].

1.2.2.5 Advantages

- a) Because of continuously fed electrode, MIG welding process is much faster as compared to TIG or stick electrode welding
- b) It can produce joints with deep penetration
- c) Thick and thin, both types of work pieces can be welded effectively
- d) Large metal deposition rates are achieved by MIG welding process
- e) The process can be easily mechanized
- f) No flux is used. MIG welding produces smooth, neat, clean and spatter free welded surfaces which require no further cleaning. This helps reducing total welding cost
- g) Higher arc travel speeds associated with MIG welding reduce distortion considerably [1].

1.2.2.6 Disadvantages

- a) The process is slightly more complex as compared to TIG or stick electrode welding because a number of variables (like electrode stick out, torch angle, welding parameters, type and size of electrode, welding torch manipulation, etc.) are required to be controlled effectively to achieve good results
- b) Welding equipment is more complex, more costly and less portable
- c) Since air drafts may disperse the shielding gas, MIG welding may not work well in outdoor welding applications
- d) Weld metal cooling rates are higher than with the processes that deposit slag over the weld metal [1].

1.2.2.7 Applications

- a) The process can be used for the welding of carbon, silicon and low alloy steels, stainless steels, aluminum, magnesium, copper, nickel, and their alloys, titanium, etc.
- b) For welding tool steels and dies
- c) For the manufacture of refrigerator parts
- d) MIG welding has been used successfully in industries like aircraft, automobile, pressure vessel, and ship building [1].



CHAPTER 2

LITERATURE REVIEW

2.1 Research Works

Weldment characteristics like penetration, bead geometry and depth of HAZ are extremely important characteristics for structural integrity. SMA welding process is used throughout the world for its simplicity and versatility. Electrode diameter, current, voltage, arc travel speed, electrode feed rate, arc length and arc spread are influential factors in deciding the weldment characteristics. The effects of these process parameters on weldment characteristics in case of SMA welding process have been studied. Bead-on-plate experiments have been conducted using a preset feed based SMA welding machine. Weldment characteristics like depth of penetration, depth of HAZ and number of undercuts, has been examined. An artificial neural network based modeling of the experiments has been successfully done to predict the patterns of results obtained from the experiments [2].

Bead geometry (bead height and width) and penetration (depth and area) are important physical characteristics of a weldment. Several welding parameters seem to affect the bead geometry and penetration. It has been observed that high arc-travel rate or low arc-power normally produced poor fusion. Higher electrode feed rate produced higher bead width making the bead flatter. Current, voltage and arc-travel rate influence the depth of penetration. The other factors that influence the penetration are heat conductivity, arc-length and arc-force. Longer arc-length produces shallower penetration. Too small arc-length may also give rise to poor penetration, if the arc-power is very low. Use of artificial neural networks to model the SMA welding process has been explored. Back-propagation neural networks have been used to associate the welding process variables with the features of the bead geometry and penetration. These networks have achieved good agreement with the training data and have yielded satisfactory generalization. A neural network could be

effectively implemented for estimating the weld bead and penetration geometric parameters [3].

Weldment characteristics like penetration, bead geometry and depth of heat affected zone are extremely important characteristics for structural integrity. Electric arc welding process is used throughout the world for its simplicity and versatility. Electrode diameter, current, voltage, arc travel speed, electrode feed rate, arc length and arc spread are influential factors in deciding the weldment characteristics. The effects of these process parameters on weldment characteristics in case of electric arc welding process have been studied. Bead on plate experiments have been conducted using a manual feed based metal arc welding machine. Weldment characteristics like depth of penetration, depth of heat affected zone and bead geometry have been examined. An artificial neural network based modeling of the experiments has been successfully done to predict the patterns of results obtained from the experiments [4].

Gas metal arc (GMA) welding process has been chosen as a metal joining technique due to the wide range of usable applications, cheap consumables and easy handling. The welding quality is generally controlled by the welding parameters. To achieve a high level of welding performance and quality, a suitable algorithm is required to fully understand the influence of welding parameters on bead geometry in the GMA welding process. An intelligent system in GMA welding processes using MATLAB/SIMULINK software has been developed. Based on multiple regressions and a neural network, the mathematical models are derived from extensive experiments with different welding parameters and complex geometrical features. The developed system enables to input the desired weld dimensions and select the optimal welding parameters. The experimental results were proved the capability of the developed system to select the welding parameters in GMA welding process according to complex external and internal geometrical features of the substrate [5].

In fusion welding process, a monolithic structure is obtained at the weldment between the two pieces to be joined. This monolithic structure called the welded zone has got different

shapes, which depend upon the type of welding process and its parameters. The strength of the welded structure depends upon the extent to which the metal penetrates between the joint and the volume of the parent metal that gets melted. The shape of the weldment governs mechanical properties of the structure. The weldment shape is generally represented by bead width, bead height and bead penetration. Neural network-based approaches have been developed to predict the locus of weld fusion zone [6].

Mathematical models are necessary to control the ever increasing automated or robotic welding processes for achieving optimum results. The effect of arc voltage, wire feed rate, welding speed, plate thickness, nozzle-to-plate distance, electrode-to-work angle and electrode polarity on weld bead geometry and shape relationship have been investigated by the statistical tool of fractional factorial technique in automatic submerged arc welding of high strength low alloy steels. The developed models have been tested for their adequacy and the coefficients were tested for their significance to arrive at the final mathematical models [7].

Automatic weld surfacing is being employed increasingly in the process and power industries. Because of its high reliability, all-position capability, ease of use, low cost and high productivity, GMAW has become a natural choice for automatic surfacing. With increasing use of GMAW in its automatic mode, there will be increased dependence on the use of equations to predict the dimensions of the weld bead. The development of such mathematical equations using a four-factor 5-level factorial technique to predict the geometry of the weld bead in the deposition of 316L stainless steel onto structural steel IS 2062 is presented. The models developed have been checked for their adequacy and significance by using the F-test and the t-test, respectively. Main and interaction effects of the control factors on dilution and bead geometry are presented in a graphical form that helps in selecting quickly the process parameters to achieve the desired quality of overlay [8].

The welding process variables of welding current, arc voltage, welding speed, gas flow rate, and offset distance, which influence weld bead shape, are coupled with each other but not directly connected with weld bead shape individually. Therefore, it is very difficult and

time consuming to determine the welding process variables necessary to obtain the desired weld bead shape. Mathematical modeling in conjunction with many experiments must be used to predict the magnitude of weld bead shape. Even though experimental results are reliable, prediction is difficult because of the coupling characteristics. The $2n - 1$ fractional factorial design method have been used to investigate the effect of welding process variables on fillet joint shape. Finally, a neural network based on the back propagation algorithm and an optimum design based on mathematical modeling has been implemented to estimate the weld parameters for the desired fillet joint shape. Mathematical modeling based on multiple nonlinear regression analysis has been used for modeling the gas metal arc welding (GMAW) parameters of the fillet joint [9].

Experimental designs technique on the experimental data available from conventional experimentation, application of neural network for predicting the weld bead geometric descriptors and use of genetic algorithm for optimization of process parameters have been explained by an integrated method with a new approach using experimental design matrix. The properties of the welded joints are affected by a large number of welding parameters. Modeling of weld bead shape is important for predicting the quality of welds. To model the welding process for predicting the bead shape parameters (also known as bead geometry parameters) of welded joints, modeling and optimization of bead shape parameters in tungsten inert gas (TIG) welding process have been developed. Multiple linear regression technique has been used to develop mathematical models for weld bead shape parameters of TIG welding process, considering the effects of main variables as well as two factor interactions. Also by using the same experimental data, an attempt has been made to predict the bead shape parameters using back-propagation neural network. To optimize the process parameters for the desired front height to front width ratio and back height to back width ratio, genetic algorithmic approach has been applied [10].

To automate a welding process, which is the present trend in fabrication industry, it is essential that mathematical models have to be developed to relate the process variables to the weld bead parameters. Because of its high reliability, deep penetration, smooth finish and high productivity, submerged arc welding (SAW) has become a natural choice in

industries for fabrication, especially for welding of pipes. Mathematical models have been developed for SAW of pipes using five level factorial techniques to predict three critical dimensions of the weld bead geometry and shape relationships. The models developed have been checked for their adequacy and significance by using the F-test and the t-test, respectively. Main and interaction effects of the process variables on bead geometry and shape factors are presented in graphical form and using which not only the prediction of important weld bead dimensions and shape relationships but also the controlling of the weld bead quality by selecting appropriate process parameter values are possible [11].

The effects of various welding parameters on welding penetration in Erdemir 6842 steel having 2.5 mm thickness welded have been investigated by robotic gas metal arc welding. The welding current, arc voltage and welding speed have been chosen as variable parameters. The depths of penetration have been measured for each specimen after the welding operations and the effects of these parameters on penetration have been researched. The welding currents have been chosen as 95, 105, 115 A, arc voltages have been chosen as 22, 24, and 26 V and the welding speeds have been chosen as 40, 60 and 80 cm/min for all experiments. It has been observed that, increasing welding current increased the depth of penetration. In addition, arc voltage is another parameter in incrimination of penetration. However, its effect is not as much as current's [12].

Welding input parameters play a very significant role in determining the quality of a weld joint. The joint quality can be defined in terms of properties such as weld-bead geometry, mechanical properties, and distortion. Generally, all welding processes are used with the aim of obtaining a welded joint with the desired weld-bead parameters, excellent mechanical properties with minimum distortion. Nowadays, application of design of experiment (DoE), evolutionary algorithms and computational network are widely used to develop a mathematical relationship between the welding process input parameters and the output variables of the weld joint in order to determine the welding input parameters that lead to the desired weld quality [13].

Considering the above literatures review, it is obvious that in one hand recently there has done a little work using MIG welding processes to observe the effects of process parameters on weldment characteristics. And in another hand it is also obvious that many researchers related with welding have been using neural network model with greater rate to compute complex calculations, as well as to predict weldment characteristics. Due to these reasons MIG welding process and Artificial Neural Network have been used in this work.

ARTIFICIAL NEURAL NETWORK

3.1 Introduction

Work on artificial neural networks, commonly referred to as “neural networks”, has been motivated right from its inception by the recognition that the human brain computes in an entirely different way from the conventional digital computer. The brain is a highly *complex, nonlinear and parallel computer* (information-processing system). It has the capability to organize its structural constituents, known as *neurons*, so as to perform certain computations (e.g., pattern recognition, perception, and motor control) many times faster than the fastest digital computer in existence today. Consider, for example, the *sonar* of a bat. Sonar is an active echo-location system. In addition to providing information about how far away a target (e.g., a flying insect) is, a bat sonar conveys information about the relative velocity of the target, the size of the target, the size of various features of the target, and the azimuth and elevation of the target (Suga,1990a,b). The complex neural computations needed to extract all this information from the target echo occur within a brain the size of a plum. Indeed, an echo-locating bat can pursue and capture its target with a facility and success rate that would be the envy of a radar or sonar engineer.

How, then, does a human brain or the brain of a bat do it? At birth, a brain has great structure and the ability to build up its own rules through what we usually refer to as “experience”. Indeed, experience is built up over time, with the most dramatic development (i.e., hard-wiring) of the human brain taking place during the first two years from birth; but the development continues well beyond that stage.

A “developing” neuron is synonymous with a plastic brain: *Plasticity* permits the developing nervous system to adapt to its surrounding environment. Just as plasticity

appears to be essential to the functioning of neurons as information-processing units in the human brain, so it is with neural networks made up of artificial neurons. In its most general form, a *neural network* is a machine that is designed to *model* the way in which the brain performs a particular task or function of interest; the network is usually implemented by using electronic components or is simulated in software on a digital computer.

To achieve good performance, neural networks employ a massive interconnection of simple computing cells referred to as “neurons” or “processing units”. We may thus offer the following definition of a neural network viewed as an adaptive machine:

A neural network is a massively parallel distributed processor made up of simple processing units, which has a natural propensity for storing experiential knowledge and making it available for use. It resembles the brain in two respects:

- 1. Knowledge is acquired by the network from its environment through a learning process.*
- 2. Interneuron connection strengths, known as synaptic weights, are used to store the acquired knowledge.*

The procedure used to perform the learning process is called a *learning algorithm*, the function of which is to modify the synaptic weights of the network in an orderly fashion to attain a desired design objective.

Neural networks are also referred to in literature as *neurocomputers*, *connectionist networks*, *parallel distributed processors*, etc. [14].

3.2 Models of a Neuron

A *neuron* is an information-processing unit that is fundamental to the operation of a neural network. The block diagram of *Figure: 3.2 (a)* show the *model* of a neuron, which forms the basis for designing (artificial) neural networks. Here we identify three basic elements of the neuronal model:

1. A set of *synapses* or *connecting links*, each of which is characterized by a *weight* or *strength* of its own. Specially, a signal x_j at the input of synapse j connected to neuron k is multiplied by the synaptic weight w_{kj} . It is important to make a note of the manner in which the subscripts of the synaptic weight w_{kj} are written. The first subscript refers to the neuron in question and the second subscript refers to the input end of the synapse to which the weight refers. Unlike a synapse in the brain, the synaptic weight of an artificial neuron may lie in a range that includes negative as well as positive values.
2. An *adder* for summing the input signals, weighted by the respective synapses of the neuron; the operations described here constitutes a *linear combiner*.
3. An *activation function* for limiting the amplitude of the output of a neuron. The activation function is also referred to as a *squashing function* in that it squashes (limits) the permissible amplitude range of the output signal to some finite value.

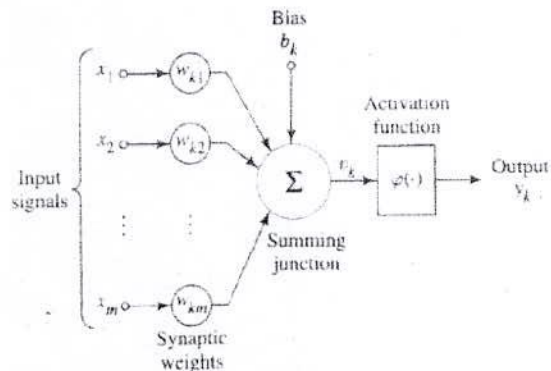


Figure: 3.2 (a) Nonlinear Model of a Neuron

Typically, the normalized amplitude range of the output of a neuron is written as the closed unit interval $[0, 1]$ or alternatively $[-1, 1]$.

The neuronal model of *Figure: 3.2 (a)* also include an externally applied *bias*, denoted by b_k . The bias b_k has the effect of increasing or lowering the net input of the activation function, depending on whether it is positive or negative, respectively.

In mathematical terms, we may describe a neuron k by writing the following pair of equations:

$$u_k = \sum_{j=1}^m w_{kj} x_j \quad (3.2.1)$$

and

$$y_k = \varphi(u_k + b_k) \quad (3.2.2)$$

Where x_1, x_2, \dots, x_m are the input signals; $w_{k1}, w_{k2}, \dots, w_{km}$ are the synaptic weights of neuron k ; u_k is the *linear combiner output* due to the input signals; b_k is the bias; $\varphi(\cdot)$ is the *activation function*; and y_k is the output signal of the neuron. The use of bias b_k has the effect of applying an *affine transformation* to the output u_k of the linear combiner in the model of *Figure: 3.2 (a)*, as shown by

$$v_k = u_k + b_k \quad (3.2.3)$$

In particular, depending on whether the bias b_k is positive or negative, the relationship between the *induced local field* or *activation potential* v_k of neuron k and the linear combiner output u_k is modified in the manner illustrated in *Figure : 3.2 (b)*; hereafter the term “induced local field” is used. Note that as a result of this affine transformation, the graph of v_k versus u_k no longer passes through the origin.

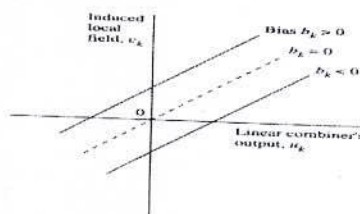


Figure: 3.2 (b) Affine Transformation produced by the presence of a bias; note that $v_k = b_k$ at $u_k=0$

The bias b_k is an external parameter of artificial neuron k . We may account for its presence as in Esq. (3.2.2). Equivalently, we may formulate the combination of Esq. (3.2.1) to (3.2.3) as follows:

$$v_k = \sum_{j=0}^m w_{kj} x_j \quad (3.2.4)$$

And

$$y_k = \varphi(v_k) \quad (3.2.5)$$

In Esq. (3.2.4) we have added a new synapse. Its input is

$$x_0 = +1 \quad (3.2.6)$$

And its weight is

$$w_{k0} = b_k \quad (3.2.7)$$

We may therefore reformulate the model of neuron k as in *Figure: 3.2 (c)*. In this figure the effect of the bias is accounted for by doing two things:

- Adding a new input signal fixed at +1.
- Adding a new synaptic weight equal to the bias b_k .

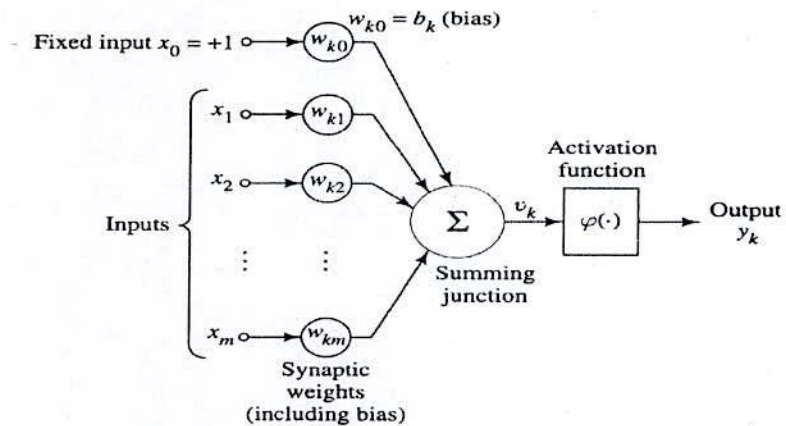


Figure: 3.2 (c) Another Nonlinear Model of a Neuron

Although the models of *Figures: 3.2 (a)* and *3.2 (c)* are different in appearance, they are mathematically equivalent [14].

3.3 Activation Function

The activation function, denoted by $\varphi(v)$, defines the output of a neuron in terms of the induced local field v . Here we identify three basic types of activation functions:

3.3.1 Threshold Function

For this type of activation function, described in *Figure: 3.3 (a)*, we have

$$\varphi(v) = \begin{cases} 1 & \text{if } v \geq 0 \\ 0 & \text{if } v < 0 \end{cases} \quad (3.3.1)$$

In engineering literature, this form of a threshold function is commonly referred to as a *Heaviside function*. Correspondingly, the output of neuron k employing such a threshold function is expressed as

$$y_k = \begin{cases} 1 & \text{if } v_k \geq 0 \\ 0 & \text{if } v_k < 0 \end{cases} \quad (3.3.2)$$

Where v_k is the induced local field of the neuron; that is,

$$v_k = \sum_{j=1}^m w_{kj} x_j + b_k \quad (3.3.3)$$

Such a neuron is referred to in the literature as the *McCulloch-Pitts model*, in recognition of the pioneering work done by McCulloch and Pitts (1943). In this model, the output of a neuron takes on the value of 1 if the induced local field of that neuron is non negative, and 0 otherwise. This statement describes the *all-or none property* of the McCulloch-Pitts model.

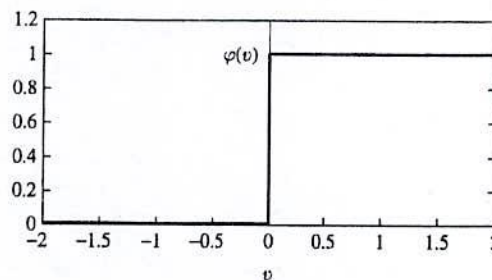


Figure: 3.3 (a) Threshold Function



3.3.2 Piecewise-Linear Function

For the piecewise-linear function described in *Figure: 3.3 (b)*, we have

$$\varphi(v) = \begin{cases} 1, & v \geq \frac{1}{2} \\ v + \frac{1}{2}, & -\frac{1}{2} < v < \frac{1}{2} \\ 0, & v \leq -\frac{1}{2} \end{cases} \quad (3.3.4)$$

Where the amplification factor inside the linear region of operation is assumed to be unity. This form of an activation function may be viewed as an *approximation* to a nonlinear amplifier.

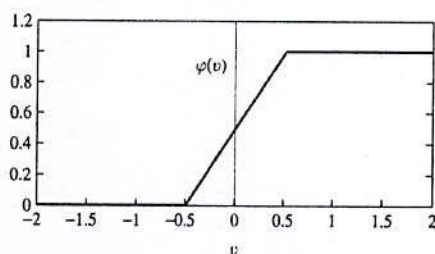


Figure: 3.3 (b) Piecewise-Linear Function

The following two situations may be viewed as special forms of the piecewise-linear function:

- A *linear combiner* arises if the linear region of operation is maintained without running into saturation.
- The piecewise-linear function reduces to a *threshold function* if the amplification factor of the linear region is made infinitely large.

3.3.3 Sigmoid Function

The sigmoid function, whose graph is s-shaped, is by far the most common form of activation function used in the construction of artificial neural networks. It is defined as a strictly increasing function that exhibits a graceful balance between linear and nonlinear behavior. An example of the sigmoid function is the *logistic function*, defined by

$$\varphi(v) = \frac{1}{1 + \exp(-av)} \quad (3.3.5)$$

where a is the *slope parameter* of the sigmoid function. By varying the parameter a , we obtain sigmoid functions of different slopes, as illustrated in *Figure: 3.3 (c)*.

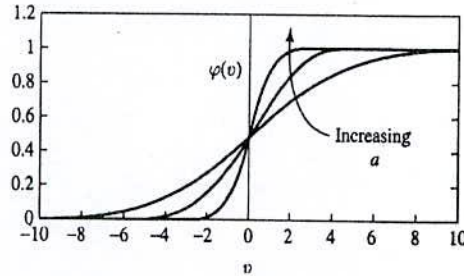


Figure: 3.3 (c) Sigmoid Function for varying slope parameter 'a'

In fact, the slope at the origin equals $a/4$. In the limit, as the slope parameter approaches infinity, the sigmoid function becomes simply a threshold function. Whereas a threshold function assumes the value of 0 or 1, a sigmoid function assumes a continuous range of values from 0 to 1. Note also that the sigmoid function is differentiable, whereas the threshold function is not.

The activation functions defined in Esq. (3.3.1), (3.3.4), and (3.3.5) range from 0 to +1. It is sometimes desirable to have the activation function range from -1 to +1, in which case the activation function assumes an antisymmetric form with respect to the origin; that is, the activation function is an odd function of the induced local field. Specially, the threshold function of Esq. (3.3.1) is now defined as

$$\varphi(v) = \begin{cases} 1 & \text{if } v > 0 \\ 0 & \text{if } v = 0 \\ -1 & \text{if } v < 0 \end{cases} \quad (3.3.6)$$

This is commonly referred to as the *signum function*. For the corresponding form of a sigmoid function we may use the *hyperbolic tangent function*, defined by

$$\varphi(v) = \tanh(v) \quad (3.3.7)$$

Allowing an activation function of the sigmoid type to assume negative values as prescribed by Esq. (3.3.7) has analytic benefits [14].

3.4 Network Architectures

The manner in which the neurons of a neural network are structured is intimately linked with the learning algorithm used to train the network. We may therefore speak of learning algorithms (rules) used in the design of neural networks as being *structured*. In general, we may identify three fundamentally different classes of network architectures:

3.4.1 Single-Layer Feed forward Networks

In a *layered* neural network the neurons are organized in the form of layers. In the simplest form of a layered network, we have an *input layer* of source nodes that projects onto an *output layer* of neurons (computations nodes), but not vice versa. In other words, this network is strictly a *feed forward* or *acyclic* type. It is illustrated in *Figure: 3.4 (a)* for the case of four nodes in both the input and output layers. Such a network is called a *single-layer network*, with the designation “single-layer” referring to the output layer of computation nodes (neurons). We do not count the input layer of source nodes because no computation is performed there.

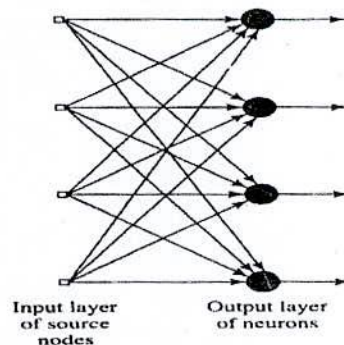


Figure: 3.4 (a) Feed forward or Acyclic Network with a Single Layer of Neurons

3.4.2 Multilayer Feed forward Networks

The second class of a feed forward neural network distinguishes itself by the presence of one or more *hidden layers*, whose computation nodes are correspondingly called *hidden neurons* or *hidden units*. The function of hidden neurons is to intervene between the external input and the network output in some useful manner. By adding one or more

hidden layers, the network is enabled to extract higher-order statistics. In a rather loose sense the network acquires a *global* perspective despite its local connectivity due to the extra set of synaptic connections and the extra dimension of neural interactions (Churchland and Sejnowski, 1992). The ability of hidden neurons to extract higher-order statistics is particularly valuable when the size of the input layer is large.

The source nodes in the input layer of the network supply respective elements of the activation pattern (input vector), which constitute the input signals applied to the neurons (computation nodes) in the second layer (i.e., the first hidden layer). The output signals of the second layer are used as inputs to the third layer, and so on for the rest of the network. Typically the neurons in each layer of the network have as their inputs the output signals of the preceding layer only. The set of output signals of the neurons in the output (final) layer of the network constitutes the overall response of the network to the activation pattern supplied by the source nodes in the input (first) layer. The architectural graph in *Figure: 3.4 (b)* illustrates the layout of a multilayer feed forward neural network for the case of a single hidden layer. For brevity the network in *Figure: 3.4 (b)* is referred to as a 10 - 4 - 2 network because it has 10 source nodes, 4 hidden neurons, and 2 output neurons. As another example, a feed forward network with m source nodes, h_1 neurons in the first hidden layer, h_2 neurons in the second hidden layer, and q neurons in the output layer is referred to as an $m-h_1-h_2-q$ network.

The neural network in *Figure: 3.4 (b)* is said to be *fully connected* in the sense that every node in each layer of the network is connected to every other node in the adjacent forward layer. If, however, some of the communication links (synaptic connections) are missing from the network, we say that the network is *partially connected*.

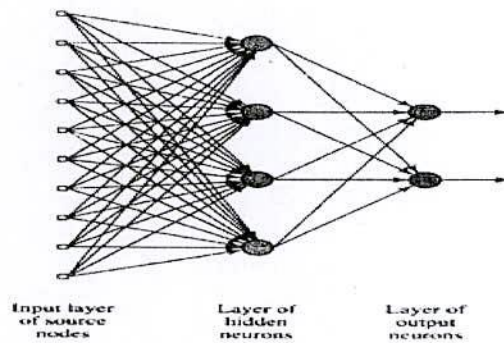


Figure: 3.4 (b) Fully Connected Feed forward or Acyclic Network with One Hidden Layer and One Output Layer

3.4.3 Recurrent Networks

A *recurrent neural network* distinguishes itself from a feed forward neural network in that it has at least one *feedback* loop. For example, a recurrent network may consist of a single layer of neurons with each neuron feeding its output signal back to the inputs of all the other neurons, as illustrated in the architectural graph in *Figure: 3.4 (c)*. In the structure depicted in this figure there are *no* self-feedback loops in the network; self-feedback refers to a situation where the output of a neuron is fed back into its own input. The recurrent network illustrated in *Figure: 3.4 (c)* also has *no* hidden neurons. In *Figure: 3.4 (d)*, we illustrate another class of recurrent networks with hidden neurons. The feedback connections shown in *Figure: 3.4 (d)* originate from the hidden neurons as well as from the output neurons.

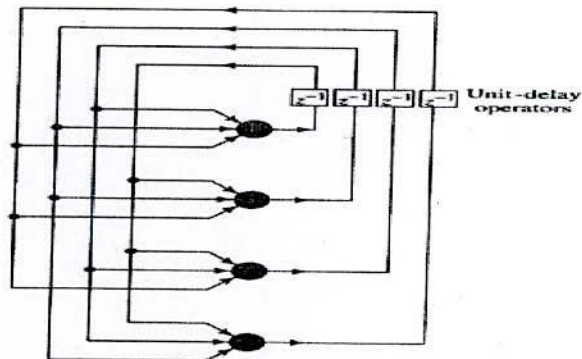


Figure: 3.4 (c) Recurrent Networks with no Self-Feedback Loops and no Hidden Neurons

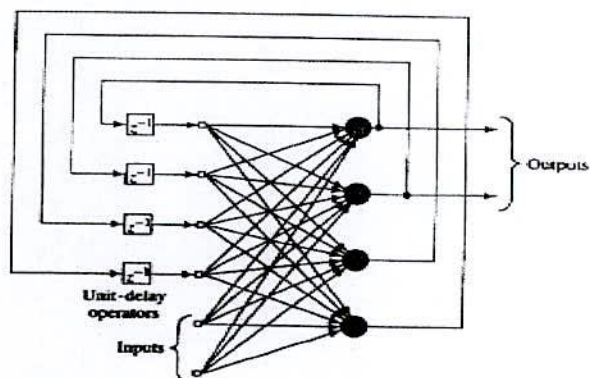


Figure: 3.4 (d) Recurrent Network with Hidden Neurons

The presence of feedback loops, whether in the recurrent structure of *Figure: 3.4 (c)* or that of *Figure: 3.4 (d)*, has a profound impact on the learning capability of the network and on its performance. Moreover, the feedback loops involve the use of particular branches composed of *unit-delay elements* (denoted by z^{-1}), which result in a nonlinear dynamical behavior, assuming that the neural network contains nonlinear units [14].

3.5 Neural Learning

We define learning in the context of neural networks, is adapted from Mendel and McClaren (1970), as:

Learning is a process by which the free parameters of a neural network are adapted through a process of stimulation by the environment in which the network is embedded. The type of learning is determined by the manner in which the parameter changes take place.

This definition of the learning process implies the following sequence of events:

- The neural network is *stimulated* by an environment.
- The neural network *undergoes changes* in its free parameters as a result of this stimulation.
- The neural network *responds in a new way* to the environment because of the changes that have occurred in its internal structure.

A prescribed set of well-defined rules for the solution of a learning problem is called a *learning algorithm*. As one would expect, there is no unique learning algorithm for the design of neural networks. Rather, we have a “kit of tools” represented by a diverse variety of learning algorithms, each of which offers advantages of its own. Basically, learning algorithms differ from each other in the way in which the adjustment to a synaptic weight of a neuron is formulated. Another factor to be considered is the manner in which a neural network (learning machine), made up of a set of interconnected neurons, relates to its environment. In this latter context we speak of a *learning paradigm* that refers to a *model* of the environment in which the neural network operates.

There have five basic learning rules:

1. Error-correction learning; it is rooted in optimum filtering.
2. Memory-based learning; it operates by memorizing the training data explicitly.

3. Hebbian learning.
4. Competitive learning.

Hebbian learning and competitive learning are both inspired by neurobiological considerations

5. Boltzmann learning; it is different because it is based on ideas borrowed from statistical mechanics.

There are three basic and fundamental learning paradigms:

1. Credit-assignment problem; which is basic to the learning process
2. Learning *with* a teacher
3. Learning *without* a teacher [14].

3.5.1 Learning with a Teacher

This is also referred to as *supervised learning*. Figure: 3.5 (a) shows a block diagram that illustrates this form of learning. In conceptual terms, we may think of the teacher as having knowledge of the environment, with that knowledge being represented by a set of *input-output examples*. The environment is, however, *unknown* to the neural network of interest. Suppose now that the teacher and the neural network are both exposed to a training vector (i.e., example) drawn from the environment. By virtue of built-in-knowledge, the teacher is able to provide the neural network with a desired response for that training vector. Indeed, the desired response represents the optimum action to be performed by the neural network. The network parameters are adjusted under the combined influence of the training vector and the error signal. The *error signal* is defined as the difference between the desired response and the actual response of the network. This adjustment is carried out iteratively in a step – by – step fashion with the aim of eventually making the neural network *emulate* the teacher; the emulation is presumed to be optimum in some statistical sense. In this way knowledge of the environment available to the teacher is transferred to the neural network through training as fully as possible. When this condition is reached, we may then dispense with the teacher and let the neural network deal with the environment completely by itself.

The form of supervised learning we have just described is the error-correction learning discussed previously. It is a closed-loop feedback system, but the unknown environment is not in the loop. As a performance measure for the system we may think in terms of the mean-square error or the sum of squared errors over the training sample, defined as a function of the free parameters of the system. This function may be visualized as a multidimensional *error-performance surface* or simply *error surface*, with the free parameters as coordinates. The true error surface is *averaged* over all possible input-output examples. Any given operation of the system under the teacher's supervision is represented as a point on the error surface.

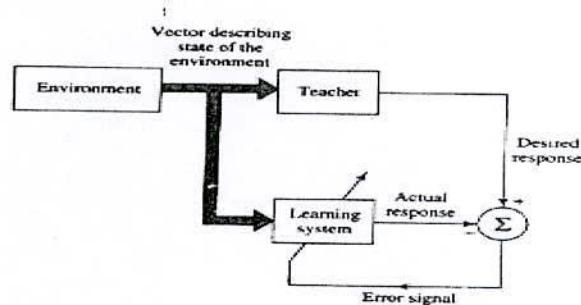


Figure: 3.5 (a) Block Diagram of a Learning with a Teacher

For the system to improve performance over time and therefore learn from the teacher, the operating has to move down successively toward a minimum point of the error surface; the minimum point may be a local minimum or a global minimum. A supervised learning system is able to do this with the useful information it has about the *gradient* of the error surface corresponding to the current behavior of the system. The gradient of an error surface at any point is a vector that points in the direction of *steepest descent*. In fact, in the case of supervised learning from examples, the system may use an *instantaneous estimate* of the gradient vector, with the example indices presumed to be those of time. The use of such an estimate results in a motion of the operating point on the error surface that is typically in the form of a “random walk”. Nevertheless, given an algorithm designed to minimize the cost function, an adequate set of input – output examples, and enough time permitted to do the training, a supervised learning system is usually able to perform such tasks as pattern classification and function approximation [14].

3.5.2 Real-Time Recurrent Learning

Real-Time Recurrent Learning algorithm derives its name from the fact that adjustments are made to the synaptic weights of a fully connected recurrent network in real time, that is, while the network continues to perform its signal processing function (Williams and Zipser, 1989). *Figure: 3.5 (b)* shows the layout of such a recurrent network. It consists of q neurons with m external inputs. The network has two distinct layers: a *concatenated input-feedback layer* and a *processing layer of computation nodes*. Correspondingly, the synaptic connections of the network are made up of feed forward and feedback connections.

The state-space model of the network is defined by the following two equations

$$\mathbf{X}(n+1) = \varphi(W_a \mathbf{x}(n) + W_b \mathbf{u}(n)) \quad (3.5.1)$$

$$\mathbf{y}(n) = \mathbf{C}\mathbf{x}(n) \quad (3.5.2)$$

where W_a is a q -by- q matrix, W_b is a q -by- $(m+1)$ matrix, \mathbf{C} is a p -by- q matrix; and $\varphi: R^q \rightarrow R^q$ is a diagonal map. The process Esq. (3.5.1) is reproduced here in the following expanded form:

$$\mathbf{x}(n+1) = \begin{bmatrix} \varphi(w_1^T \xi(n)) \\ \cdot \\ \varphi(w_j^T \xi(n)) \\ \cdot \\ \varphi(w_q^T \xi(n)) \end{bmatrix} \quad (3.5.3)$$

where it is assumed that all the neurons have a common activation function $\varphi(\cdot)$. The $(q+m+1)$ -by-1 vector w_j is the synaptic weight vector of neuron j in the recurrent network, that is,

$$w_j = \begin{bmatrix} w_{a,j} \\ w_{b,j} \end{bmatrix}, \quad j = 1, 2, \dots, q \quad (3.5.4)$$

where $w_{a,j}$ and $w_{b,j}$ are the j th columns of the transposed weight matrices W_a^T and W_b^T , respectively. The $(q+m+1)$ -by-1 vector $\xi(n)$ is defined by

$$\xi(n) = \begin{bmatrix} x(n) \\ u(n) \end{bmatrix} \quad (3.5.5)$$

where $\mathbf{x}(n)$ is the q -by-1 state vector and $\mathbf{u}(n)$ is the $(m + 1)$ -by-1 input vector. The first element of $\mathbf{u}(n)$ is +1 and, in a corresponding way, the first element of $\mathbf{w}_{b,j}$ is equal to the bias b_j applied to neuron j .

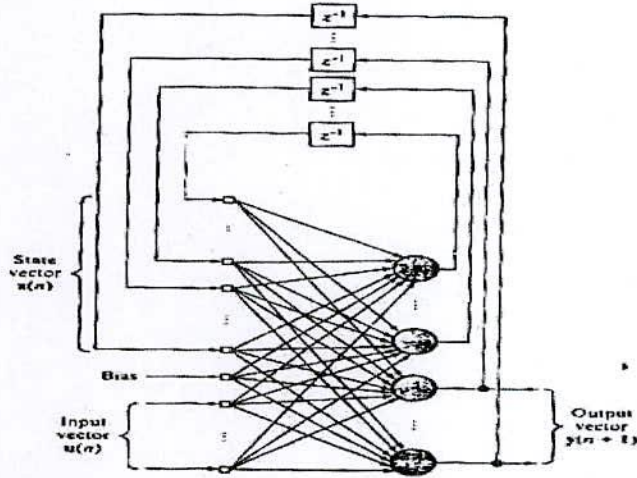


Figure: 3.5 (b) Fully connected recurrent network for formulation of the RTRL algorithm

To simplify the presentation, we introduce three new matrices $\Lambda_j(n)$, $\mathbf{U}_j(n)$ and $\Phi(n)$, described as follows:

1. $\Lambda_j(n)$ is a q -by- $(q + m + 1)$ matrix defined as the partial derivative of the state vector $\mathbf{x}(n)$ with respect to the weight vector \mathbf{w}_j :

$$\Lambda_j(n) = \frac{\partial \mathbf{x}(n)}{\partial \mathbf{w}_j}, \quad j = 1, 2, \dots, q \quad (3.5.6)$$

2. $\mathbf{U}_j(n)$ is a $(q + m + 1)$ matrix whose rows are all zero, except for the j th row that is equal to the transpose of vector $\xi(n)$:

$$\mathbf{U}_j(n) = \begin{bmatrix} 0 \\ \xi^T(n) \\ 0 \end{bmatrix} \leftarrow j\text{th row, } j = 1, 2, \dots, q \quad (3.5.7)$$

3. $\Phi(n)$ is a q -by- q diagonal matrix whose k th diagonal element is the partial derivative of the activation function with respect to its argument, evaluated at $w_j^T \xi(n)$:

$$\Phi(n) = \text{diag}(\varphi'(w_1^T \xi(n)), \dots, \varphi'(w_j^T \xi(n)), \dots, \varphi'(w_q^T \xi(n))) \quad (3.5.8)$$

With these definitions, we may now differentiate Esq. (3.5.3) with respect to w_j . Then, using the chain rule of calculus, we obtain the following recursive equation:

$$\Lambda_j(n+1) = \Phi(n) [W_a(n)\Lambda_j(n) + U_j(n)], \quad j = 1, 2, \dots, q \quad (3.5.9)$$

This recursive equation describes the *nonlinear state dynamics* (i.e., evolution of the state) of the real-time recurrent learning process.

To complete the description of this learning process, we need to relate the matrix $\Lambda_j(n)$ to the gradient of the error surface with respect to w_j . To do this, we first use the measurement Esq. (3.5.2) to define the p -by-1 error vector:

$$\begin{aligned} \mathbf{e}(n) &= \mathbf{d}(n) - \mathbf{y}(n) \\ &= \mathbf{d}(n) - \mathbf{C}\mathbf{x}(n) \end{aligned} \quad (3.5.10)$$

The instantaneous sum of squared errors at time n is defined in terms of $\mathbf{e}(n)$ by

$$E(n) = \frac{1}{2} \mathbf{e}^T(n) \mathbf{e}(n) \quad (3.5.11)$$

The objective of the learning process is to minimize a cost function obtained by summing $E(n)$ over all time n ; that is,

$$E_{\text{total}} = \sum_n E(n)$$

To accomplish this objective we may use the method of steepest descent, which requires knowledge of the *gradient matrix*, written as

$$\begin{aligned} \nabla_w E_{\text{total}} &= \frac{\partial}{\partial \mathbf{W}} E_{\text{total}} \\ &= \sum_n \frac{\partial}{\partial \mathbf{W}} E(n) \\ &= \sum_n \nabla_w E(n) \end{aligned}$$

where $\nabla_w E(n)$ is the gradient of $E(n)$ with respect to the weight matrix $\mathbf{W} = \{w_k\}$. We may, if desired, continue with this equation and derive update equations for the synaptic weights of the recurrent network without invoking approximations. However, in order to develop a learning algorithm that can be used to train the recurrent network in *real time*, we

must use an instantaneous *estimate* of the gradient, namely $\nabla_w E(n)$, which results in an *approximation* to the method of steepest descent.

Returning to Esq. (3.25) as the cost function to be minimized, we differentiate it with respect to the weight vector w_j , obtaining

$$\begin{aligned} \frac{\partial}{\partial w_j} E(n) &= \left(\frac{\partial e(n)}{\partial w_j} \right) e(n) \\ &= -C \left(\frac{\partial x(n)}{\partial w_j} \right) e(n) \\ &= -C \Lambda_j(n) e(n), \quad j = 1, 2, \dots, q \end{aligned} \quad (3.5.12)$$

The adjustment applied to synaptic weight vector $w_j(n)$ of neuron j is therefore determined by

$$\begin{aligned} \Delta w_j(n) &= -\eta \frac{\partial}{\partial w_j} E(n) \\ &= \eta C \Lambda_j(n) e(n), \quad j = 1, 2, \dots, q \end{aligned} \quad (3.5.13)$$

where η is the learning-rate parameter and $\Lambda_j(n)$ is itself governed by Esq. (3.23).

The only remaining item is that of specifying the *initial conditions* to start the learning process. For this purpose we set

$$\Lambda_j(0) = 0 \quad \text{for all } j \quad (3.5.14)$$

the implication of which is that initially the recurrent network resides in a constant state.

Table: 3.5 presents a summary of the real-time recurrent learning algorithm. The formulation of the algorithm as described here applies to an arbitrary activation function $\varphi(\cdot)$ that is differentiable with respect to its argument. For the special case of a sigmoidal nonlinearity in the form of a hyperbolic tangent function, we have

$$\begin{aligned} x_j(n+1) &= \varphi(v_j(n)) \\ &= \tanh(v_j(n)) \end{aligned}$$

and



$$\begin{aligned}
 \varphi'(v_j(n)) &= \frac{\partial \varphi(v_j(n))}{\partial v_j(n)} \\
 &= \text{sech}^2(v_j(n)) \\
 &= 1 - x_j^2(n+1)
 \end{aligned}
 \tag{3.5.15}$$

where $v_j(n)$ is the induced local field of neuron j and $x_j(n+1)$ is its state at $n+1$.

Table: 3.5 Summary of the Real-Time Recurrent Learning Algorithm

<p><i>Parameters:</i> m = dimensionality of input space q = dimensionality of state space p = dimensionality of output space w_j = synaptic weight vector of neuron $j, = 1, 2, \dots, q$.</p> <p><i>Initialization:</i></p> <ol style="list-style-type: none"> 1. Set the synaptic weights of the algorithm to small values selected from a uniform distribution. 2. Set the initial value of the state vector $\mathbf{x}(0) = \mathbf{0}$. 3. Set $\Lambda_j(0) = \mathbf{0}$ for $j = 1, 2, \dots, q$. <p><i>Computations:</i> Compute for $n = 0, 1, 2, \dots$,</p> $\Lambda_j(n+1) = \Phi(n) [W_a(n)\Lambda_j(n) + U_j(n)]$ $\mathbf{e}(n) = \mathbf{d}(n) - \mathbf{C}\mathbf{x}(n)$ $\Delta w_j(n) = \eta \mathbf{C} \Lambda_j(n) \mathbf{e}(n)$ <p>The definitions of $\mathbf{x}(n)$, $\Lambda_j(n)$, $U_j(n)$ and $\Phi(n)$ are given in Esq. (3.17), (3.20), (3.21), and (3.22). respectively.</p>
--

The use of the instantaneous gradient $\nabla_w E(n)$ means that the real-time recurrent learning algorithm described here deviates from a non-real-time one based on the true gradient $\nabla_w E_{\text{total}}$. While the real-time recurrent learning algorithm is not guaranteed to follow the precise negative gradient of the total error function $E_{\text{total}}(\mathbf{W})$ with respect to the weight matrix \mathbf{W} , the practical differences between the real-time and non-real-time versions are often slight; these two versions become nearly identical as the learning-rate parameter η is reduced. The most severe potential consequence of this deviation from the true gradient-following behavior is that the observed trajectory (obtained by plotting $E(n)$ versus the

elements of the weight matrix $\mathbf{W}(n)$ may itself depend on the weight changes produced by the algorithm, which may be viewed as another source of feedback and therefore a cause of instability in the system. We can avoid this effect by using a learning-rate parameter η small enough to make the time scale of the weight changes much smaller than the time scale of the network operation (Williams and Zipser, 1989) [14].

CHAPTER 4

PROCEDURES / METHODOLOGY

4.1 Introduction

Experimental Procedure/Methodology is nothing but the adopted processes and the sequence of those are known as experimental procedure/methodology. In this research work the considered processes and their sequences are as follows:

- Selection and preparation of specimens
- Selection the necessary machines & workshops
- Selection the variable process parameters
- Selection the weldment characteristics to be measured
- Perform welding to make bead on the specimens
- Measuring and recording the process parameters variations
- Measuring and recording the weldment characteristics values as experimental results
- Computing through an Artificial Neural Network Model (using Real-Time Recurrent Learning algorithm) and recording the weldment characteristics values as computational results
- Comparing the experimental values with the computational values.

4.2 Experimental Procedures

Medium carbon steel plate of 12 mm thickness has been chosen as base metal upon which welding has been performed. 120 pieces of size 150 mm × 75 mm has been cut away from a large flat plate using oxy-acetylene flame as specimens. The specimens then cleaned before welding.

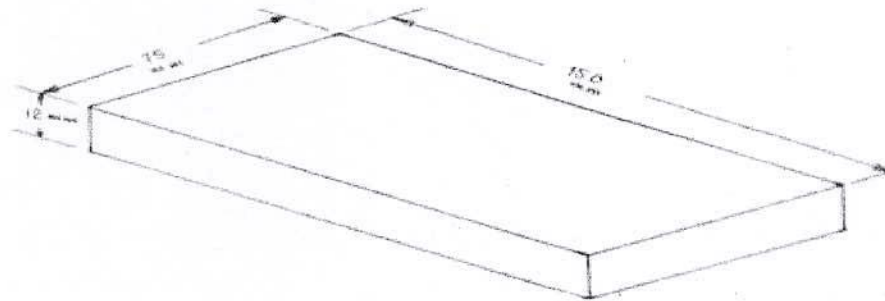


Figure: 4.2 (a) Sketch of Specimen with Dimensional Configuration

To perform welding (i.e., a straight bead on the flat surface of specimens) Transmig 350C semi-automatic MIG Welding machine of MUREX company of England has been chosen. Welding workshop of Hope Technical Institute, Khulna has been selected and their welding teacher has been chosen as welder. To prepare the specimen, perform welding (single and straight bead on surface of the specimen) and to measure the weldment characteristics except hardness - the welding shop and the metallurgy laboratory of Mechanical Engineering Department of Khulna University of Engineering & Technology, Khulna; to measure the Rockwell hardness - Bangladesh Industry and Technical Assistance Center (BITAC), Khulna have been used.

Process parameters are nothing but some conditions, which are maintain during welding process. With variety of welding process to process these parameters means conditions will vary. In a typical welding process there may choose a lot of parameters. But it should have

mind that, in a typical welding process every parameters variation have very significant effects on weldment characteristics.

However, in MIG welding process the followings may consider as *process parameters*:

- Metal of work piece & electrode wire
- Electrode wire diameter
- Electrode wire feed rate
- Used inert gas
- Gas supply pressure
- Electrode polarity
- Arc spread
- Thickness of work piece
- Welding current
- Welding speed (table or hand speed)
- Arc length
- Welding voltage
- Arc start process
- Electrode-to-work angle
- Welding joint preparation

In this research work the followings have been considered as major process parameters –

- Electrode wire diameter
- Current in ampere
- Electrode wire feed rate

Considering the welding machine capability and facility, requirement for this work and availability of other facilities the following process parameters values have been finally selected as input variables:

- 0.8 & 1.0 mm diameter medium carbon steel electrode wire
- 20 step welding current between 194 - 340 amp range
- 4600 & 5600 mm/min electrode wire feed rate.

More or less the following process parameters have been considered as constant throughout the entire experiment, e.g., welding speed around 140 mm/min, arc length around 3 mm, carbon dioxide (CO₂) gas have been used as inert gas, gap length in between nozzle and

plate have been maintained in the range of 5 – 7 mm and electrode angle have been maintained in the range of 65° – 75° .

Again weldment characteristics are nothing but some quality of weldment means welded zone or jointed zone.

And *weldment characteristics* may consider as follows:

- Bead width
- Depth of penetration
- Hardness of penetrated zone
- Metallurgy of penetrated zone
- Spattering rate
- Bending strength of bead
- Bead height or reinforcement
- Depth of heat affected zone
- Metallurgy of reinforcement
- Number of undercuts
- Tensile strength of bead
- Weldment appearance
- Crack or blow hole or porosity producing rate into the molten zone

In this research work the followings have been considered as weldment characteristics –

- Bead Width
- Depth of Penetration
- Bead Height
- Depth of HAZ
- Hardness of penetrated zone

After marking the specimens using number punch to give identity as sample serial number, a straight bead has made along the middle line of width on the surface of the specimens. During this all considered process parameter variations according to sample serial number have been recorded.

About 50 mm long pieces have been cut away from the middle position of the straight bead from every welded piece and have been taken for further experiment. The two ends along straight bead of those pieces have grinded with pedestal grinding machine, polished with 0, 2, 3, 4 grade emery paper and lastly with polishing machine embraced with cloth.

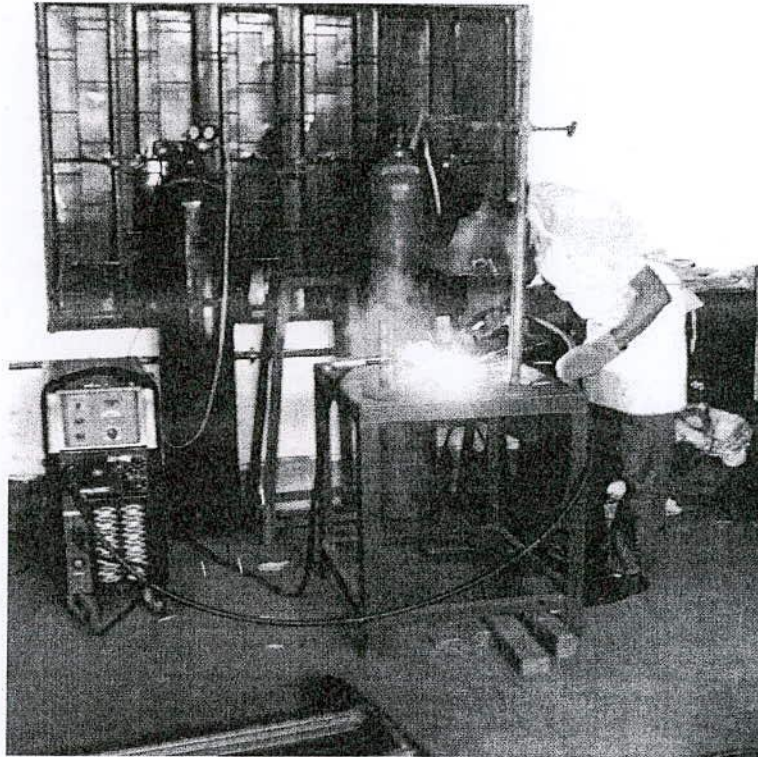


Figure: 4.2 (b) Photograph of MIG Welding operation

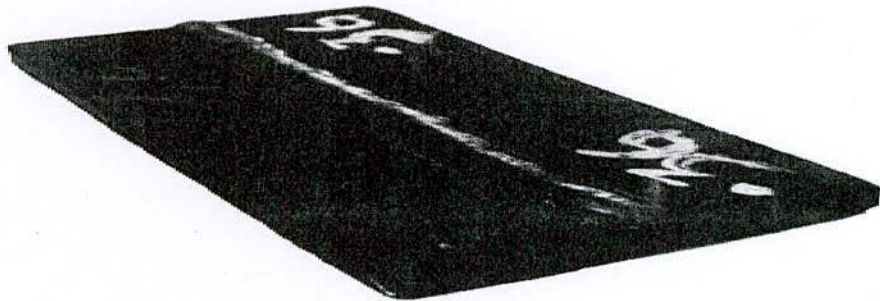


Figure: 4.2 (c) Photograph of Weldment

After performing required polishing of both ends properly, etched with 5% nitric acid solution (Nital) and then bead width, bead height, depth of penetration, depth of HAZ have been measured with digital slide caliper and recorded.

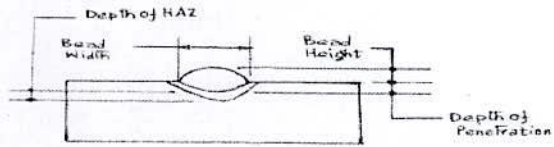


Figure: 4.2 (d) Sketch of Weld Bead Geometry and Heat Affected Zone

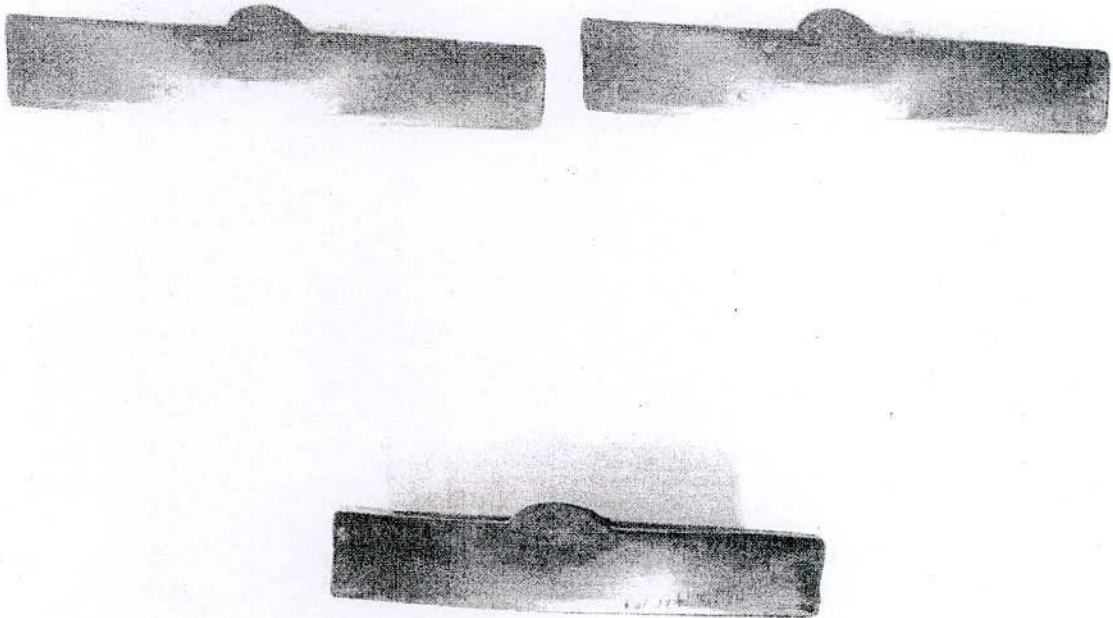


Figure: 4.2 (e) Photograph of Bead Width, Bead Height, Penetrated and Heat Affected Zone of Weldment.

After this, using Rockwell hardness testing machine, hardness number of penetrated zone of every pieces have been taken on C scale and recorded. Then the average 40 reasonable values have been taken for further computation purpose through ANN model, because three pieces have been taken as a set of specimens.

After finishing the all experimental tasks, used process parameters values and measured weldment characteristics values have been recorded as experimental results along with the

sample serial numbers in tabular form. And after performing computational tasks through Real-Time Recurrent Learning algorithm, used process parameters values and obtained weldment characteristics values have been recorded as computational results along with the sample serial numbers in tabular form also.

In 'CHAPTER 5 Results and Discussions' the results in tabular form have been given and comparison in between experimental and computational values have been illustrated in graphical form also.

CHAPTER 5

RESULTS AND DISCUSSIONS

5.1 Results

The experimental and computational values of weldment characteristics, which have been obtained respectively from the experiments using different process parameters variation and through ANN model using experimental values of process parameters as well as weldment characteristics as inputs, have been recorded separately and given in the subsequent tables.

The comparison in between the experimental and computational values with same process parameters variation have been given as graphical form in the subsequent figures also.

5.1.1 Experimental Results

Table: 5.1 (a) Values of Bead Width, Bead Height, Depth of Penetration & Heat Affected Zone and Hardness using current range from 194 – 263 amps for electrode wire diameter and feed rate respectively 0.8 mm and 4600 mm/min.

Sample Serial No.	Process Parameters			Weldment Characteristics				
	Wire Dias (mm)	Wire feed rate (mm/min)	Welding current (amp)	Bead Width (mm)	Bead Height (mm)	Depth of Penetration (mm)	Depth of HAZ (mm)	Hardness of Weldment
1	0.8	4600	194	7.00	3.50	1.50	1.50	20.00
5	0.8	4600	202	7.00	3.50	1.50	1.50	20.00
8	0.8	4600	209	7.50	3.50	2.00	1.50	25.00
12	0.8	4600	217	7.50	3.50	2.00	1.50	20.00
15	0.8	4600	225	8.00	3.50	2.00	2.00	25.00
47	0.8	4600	232	8.50	3.50	2.50	2.50	15.00
50	0.8	4600	240	9.00	3.50	2.50	2.00	20.00
53	0.8	4600	248	9.50	3.00	2.50	2.00	20.00
56	0.8	4600	255	10.00	3.00	2.50	2.00	15.00
59	0.8	4600	263	10.00	3.00	2.50	2.00	20.00

Table: 5.1 (b) Values of Bead Width, Bead Height, Depth of Penetration & Heat Affected Zone and Hardness using current range from 271 – 340 amp for electrode wire diameter and feed rate respectively 0.8 mm and 5600 mm/min.

Sample Serial No.	Process Parameters			Weldment Characteristics				
	Wire Dias (mm)	Wire feed rate (mm/min)	Welding current (amp)	Bead Width (mm)	Bead Height (mm)	Depth of Penetration (mm)	Depth of HAZ (mm)	Hardness of Weldment
32	0.8	5600	271	11.00	3.50	2.50	2.00	20.00
34	0.8	5600	278	11.00	3.50	2.50	2.00	20.00
38	0.8	5600	286	11.00	3.50	2.50	2.50	20.00
42	0.8	5600	294	11.50	3.00	3.00	2.50	15.00
44	0.8	5600	302	11.50	3.00	3.00	2.00	20.00
18	0.8	5600	309	12.00	3.00	3.00	3.00	10.00
21	0.8	5600	317	12.50	3.00	3.00	3.00	15.00
22	0.8	5600	325	12.50	3.00	3.50	3.00	15.00
25	0.8	5600	332	13.00	3.00	3.50	3.00	15.00
29	0.8	5600	340	13.00	3.00	3.00	3.00	10.00

Table: 5.1 (c) Values of Bead Width, Bead Height, Depth of Penetration & Heat Affected Zone and Hardness using current range from 194 – 263 amp for electrode wire diameter and feed rate respectively 1.0 mm and 4600 mm/min.

Sample Serial No.	Process Parameters			Weldment Characteristics				
	Wire Dias (mm)	Wire feed rate (mm/min)	Welding current (amp)	Bead Width (mm)	Bead Height (mm)	Depth of Penetration (mm)	Depth of HAZ (mm)	Hardness of Weldment
62	1.0	4600	194	8.00	4.00	2.00	1.50	20.00
64	1.0	4600	202	8.00	4.00	2.00	1.50	20.00
69	1.0	4600	209	10.00	4.00	2.50	2.00	20.00
71	1.0	4600	217	10.00	4.00	2.50	2.00	25.00
74	1.0	4600	225	11.00	4.00	3.00	2.00	20.00
77	1.0	4600	232	12.50	4.50	3.00	2.50	15.00
81	1.0	4600	240	12.50	4.50	3.00	2.00	20.00
83	1.0	4600	248	12.50	4.00	3.50	2.50	20.00
86	1.0	4600	255	13.50	3.50	3.50	2.50	20.00
89	1.0	4600	263	13.50	3.50	3.50	2.50	15.00

Table: 5.1 (d) Values of Bead Width, Bead Height, Depth of Penetration & Heat Affected Zone and Hardness using current from range 271 – 340 amp for electrode wire diameter and feed rate respectively 1.0 mm and 5600 mm/min.

Sample Serial No.	Process Parameters			Weldment Characteristics				
	Wire Dias (mm)	Wire feed rate (mm/min)	Welding current (amp)	Bead Width (mm)	Bead Height (mm)	Depth of Penetration (mm)	Depth of HAZ (mm)	Hardness of Weldment
93	1.0	5600	271	14.00	4.00	2.50	3.00	15.00
96	1.0	5600	278	14.50	4.00	2.50	3.00	10.00
97	1.0	5600	286	15.00	4.00	3.50	2.50	20.00
101	1.0	5600	294	15.00	3.00	3.00	3.00	15.00
103	1.0	5600	302	15.00	3.50	3.00	2.50	20.00
108	1.0	5600	309	15.50	3.00	3.00	2.50	20.00
111	1.0	5600	317	15.50	3.00	3.50	3.50	20.00
113	1.0	5600	325	16.00	3.00	2.50	3.50	15.00
115	1.0	5600	332	16.00	3.00	3.00	3.50	15.00
119	1.0	5600	340	16.00	2.50	3.00	2.50	10.00



5.1.2 Computational Results

Table: 5.1 (e) Values of Bead Width, Bead Height, Depth of Penetration & Heat Affected Zone and Hardness using current range from 194 – 263 amp for electrode wire diameter and feed rate respectively 0.8 mm and 4600 mm/min.

Sample Serial No.	Process Parameters			Weldment Characteristics				
	Wire Dias (mm)	Wire feed rate (mm/min)	Welding current (amp)	Bead Width (mm)	Bead Height (mm)	Depth of Penetration (mm)	Depth of HAZ (mm)	Hardness of Weldment
1	0.8	4600	194	7.0251	3.5782	1.5156	1.5251	20.9130
5	0.8	4600	202	7.0369	3.5693	1.5149	1.5328	20.7557
8	0.8	4600	209	7.5288	3.5328	2.0243	1.5386	24.7171
12	0.8	4600	217	7.5327	3.5125	2.0251	1.5397	20.0124
15	0.8	4600	225	8.0423	3.5122	2.0235	1.9835	25.2629
47	0.8	4600	232	8.5478	3.5113	2.5109	2.0375	15.5724
50	0.8	4600	240	9.0492	3.5087	2.5207	2.0247	19.7470
53	0.8	4600	248	9.5287	3.0763	2.5225	2.0364	19.8871
56	0.8	4600	255	10.0639	3.0385	2.5233	2.0428	15.1108
59	0.8	4600	263	10.0471	3.0238	2.5247	2.0482	19.2022

Table: 5.1 (f) Values of Bead Width, Bead Height, Depth of Penetration & Heat Affected Zone and Hardness using current range from 271 – 340 amp for electrode wire diameter and feed rate respectively 0.8 mm and 5600 mm/min.

Sample Serial No.	Process Parameters			Weldment Characteristics				
	Wire Dias (mm)	Wire feed rate (mm/min)	Welding current (amp)	Bead Width (mm)	Bead Height (mm)	Depth of Penetration (mm)	Depth of HAZ (mm)	Hardness of Weldment
32	0.8	5600	271	11.0729	3.5293	2.5332	2.0351	19.9796
34	0.8	5600	278	11.0467	3.5182	2.5126	2.0384	19.9672
38	0.8	5600	286	11.0821	3.4751	2.5189	2.5297	19.2199
42	0.8	5600	294	11.5934	3.0187	2.9813	2.5327	15.3415
44	0.8	5600	302	11.5626	3.0152	2.9887	2.0348	19.4382
18	0.8	5600	309	12.0345	3.0129	2.9912	2.9832	10.6328
21	0.8	5600	317	12.5573	3.0151	3.0412	2.9827	15.7019
22	0.8	5600	325	12.5828	2.9864	3.4896	2.9845	15.7675
25	0.8	5600	332	13.0652	2.9752	3.4537	3.0556	15.9533
29	0.8	5600	340	13.0981	2.9678	3.4695	3.0823	10.0337

Table: 5.1 (g) Values of Bead Width, Bead Height, Depth of Penetration & Heat Affected Zone and Hardness using current range from 194 – 263 amp for electrode wire diameter and feed rate respectively 1.0 mm and 4600 mm/min.

Sample Serial No.	Process Parameters			Weldment Characteristics				
	Wire Dias (mm)	Wire feed rate (mm/min)	Welding current (amp)	Bead Width (mm)	Bead Height (mm)	Depth of Penetration (mm)	Depth of HAZ (mm)	Hardness of Weldment
62	1.0	4600	194	8.0326	4.0127	2.0167	1.5298	20.9353
64	1.0	4600	202	8.0434	4.0495	2.0249	1.5486	20.3198
69	1.0	4600	209	9.9424	3.9765	2.4876	1.9785	20.7426
71	1.0	4600	217	9.9365	3.9537	2.4917	1.9637	20.0397
74	1.0	4600	225	10.9572	3.9821	2.8873	1.9465	20.2920
77	1.0	4600	232	12.4358	4.4983	2.9185	2.5425	15.6029
81	1.0	4600	240	12.4208	4.4897	2.9367	2.0521	19.7789
83	1.0	4600	248	12.4455	3.9873	3.4873	2.5607	19.9204
86	1.0	4600	255	13.4217	3.4827	3.4913	2.5354	19.1451
89	1.0	4600	263	13.3854	3.4801	3.4987	2.4598	15.2374

Table: 5.1 (h) Values of Bead Width, Bead Height, Depth of Penetration & Heat Affected Zone and Hardness using current range from 271 – 340 amp for electrode wire diameter and feed rate respectively 1.0 mm and 5600 mm/min.

Sample Serial No.	Process Parameters			Weldment Characteristics				
	Wire Dias (mm)	Wire feed rate (mm/min)	Welding current (amp)	Bead Width (mm)	Bead Height (mm)	Depth of Penetration (mm)	Depth of HAZ (mm)	Hardness of Weldment
93	1.0	5600	271	13.9257	3.9835	2.5378	2.9638	15.8096
96	1.0	5600	278	14.4308	3.9723	2.5286	2.9752	10.0992
97	1.0	5600	286	14.9165	3.9687	3.4827	2.5345	19.2533
101	1.0	5600	294	14.9202	3.0185	2.9138	2.9348	15.3761
103	1.0	5600	302	14.8705	3.5297	2.9562	2.4936	19.4737
108	1.0	5600	309	15.4726	3.0141	2.9593	2.5136	19.6690
111	1.0	5600	317	15.3872	3.0178	3.4897	3.5315	19.7385
113	1.0	5600	325	15.9217	2.9873	2.5134	3.4883	15.8042
115	1.0	5600	332	15.9183	2.9756	3.0183	3.4927	15.9898
119	1.0	5600	340	15.8924	2.5274	3.0127	2.6127	10.0696

5.1.3 Comparisons ('Computational' have replaced with 'Predicted' in the following figures)

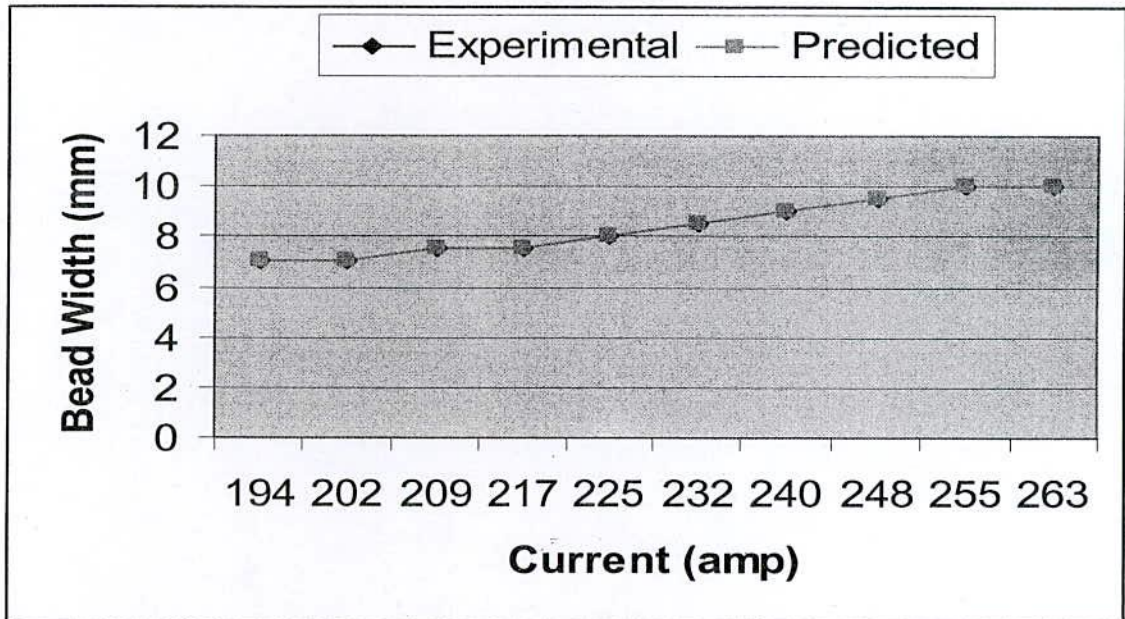


Figure: 5.1 (a) Comparison of Bead Width values using current range from 194 – 263 amps, electrode wire diameter and feed rate respectively 0.8 mm and 4600 mm/min.

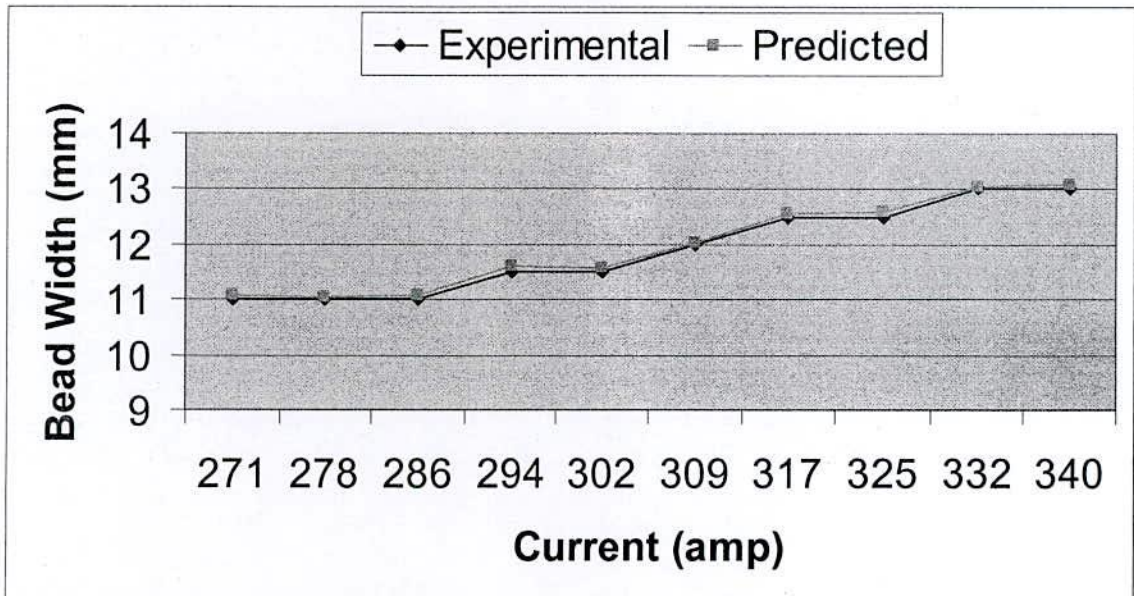


Figure: 5.1 (b) Comparison of Bead Width values using current range from 271 - 340 amps, electrode wire diameter and feed rate respectively 0.8 mm and 5600 mm/min.

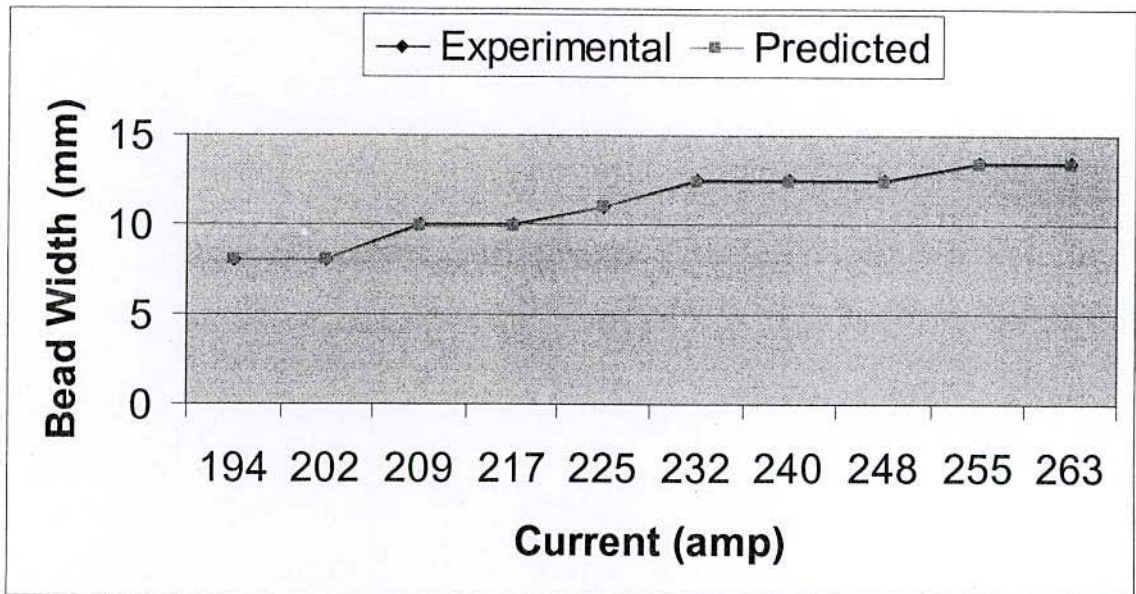


Figure: 5.1 (c) Comparison of Bead Width values using current range from 194 - 263 amps, electrode wire diameter and feed rate respectively 1.0 mm and 4600 mm/min.

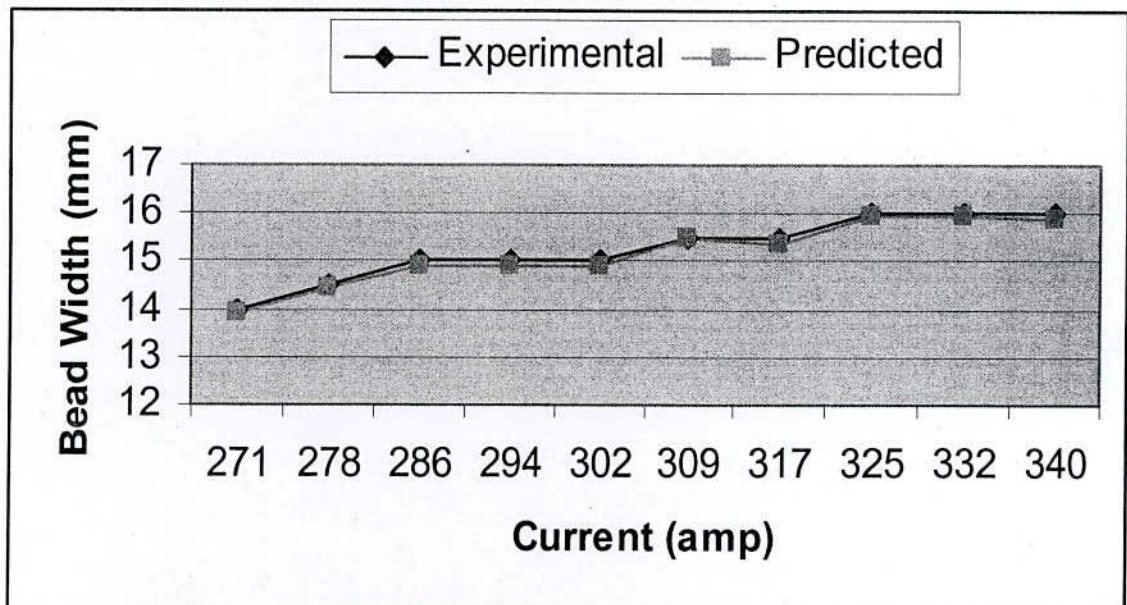


Figure: 5.1 (d) Comparison of Bead Width values using current range from 271 - 340 amps, electrode wire diameter and feed rate respectively 1.0 mm and 5600 mm/min.

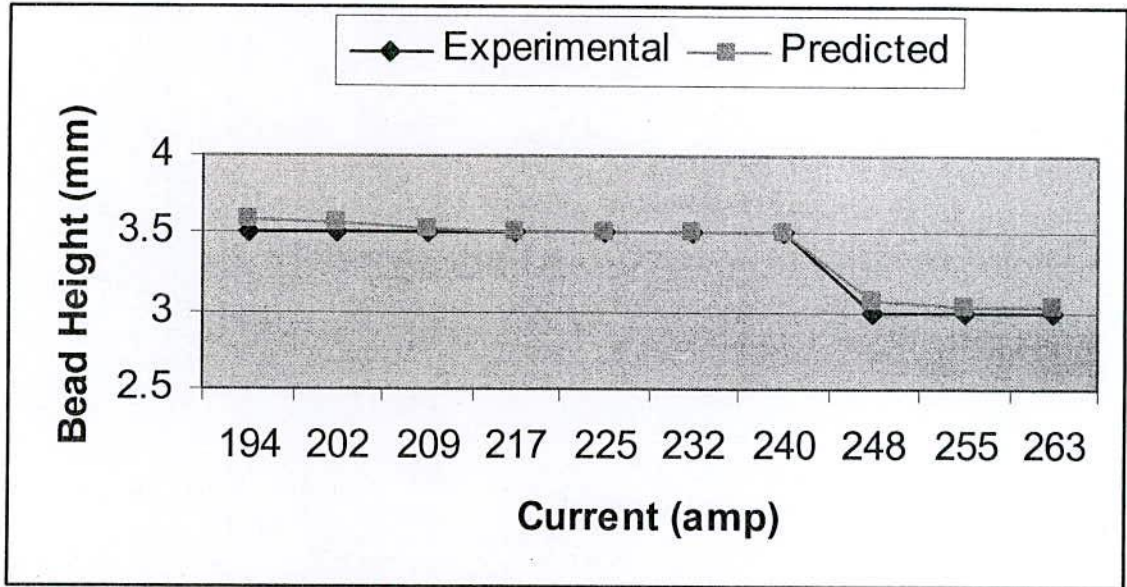


Figure: 5.1 (e) Comparison of Bead Height values using current range from 194 - 263 amps, electrode wire diameter and feed rate respectively 0.8 mm and 4600 mm/min.

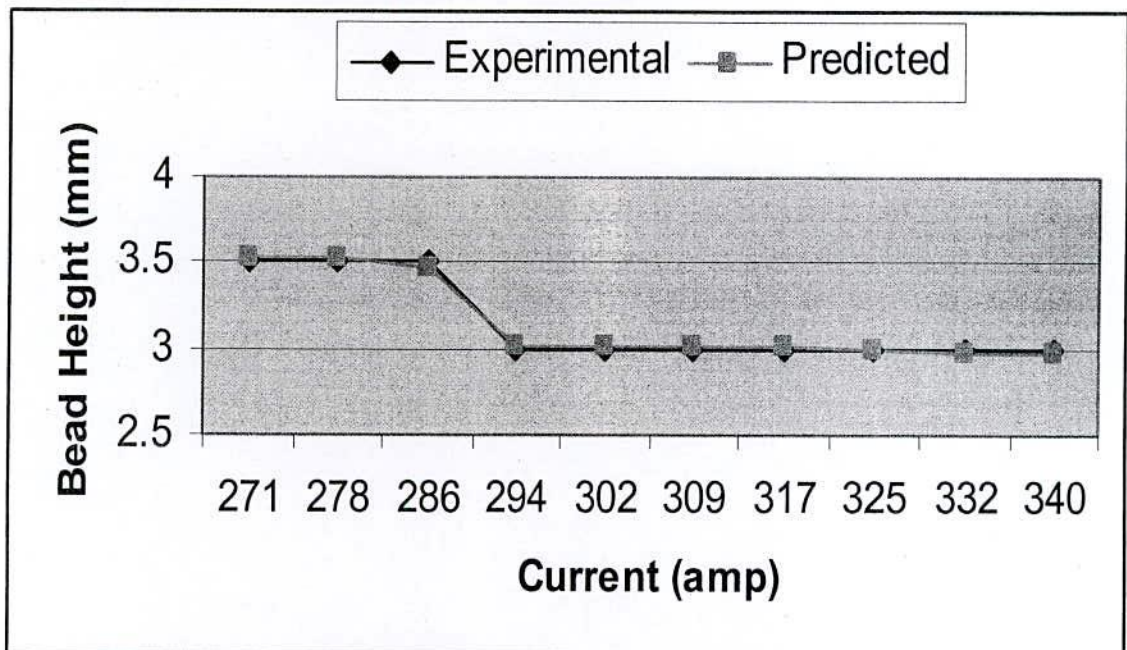


Figure: 5.1 (f) Comparison of Bead Height values using current range from 271 - 340 amps, electrode wire diameter and feed rate respectively 0.8 mm and 5600 mm/min.

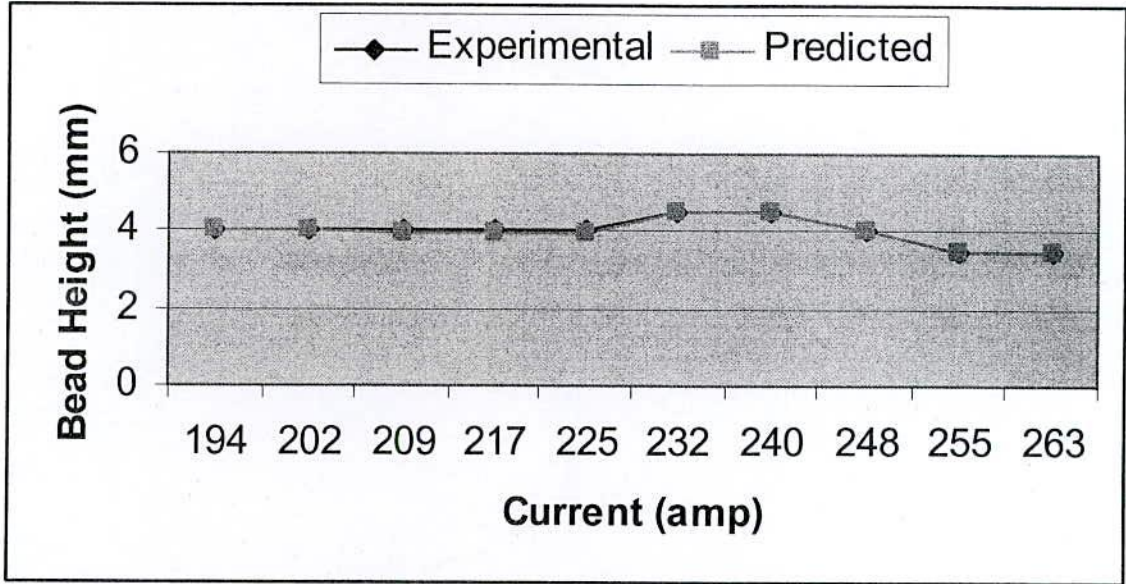


Figure: 5.1 (g) Comparison of Bead Height values using current range from 194 - 263 amps, electrode wire diameter and feed rate respectively 1.0 mm and 4600 mm/min.

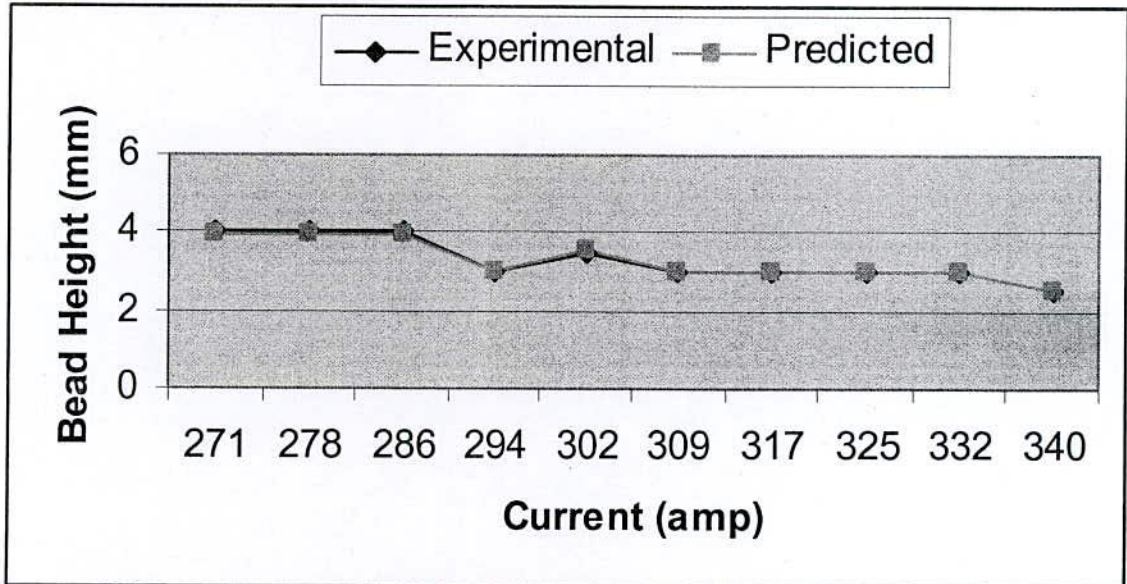


Figure: 5.1 (h) Comparison of Bead Height values using current range from 271 - 340 amps, electrode wire diameter and feed rate respectively 1.0 mm and 5600 mm/min.

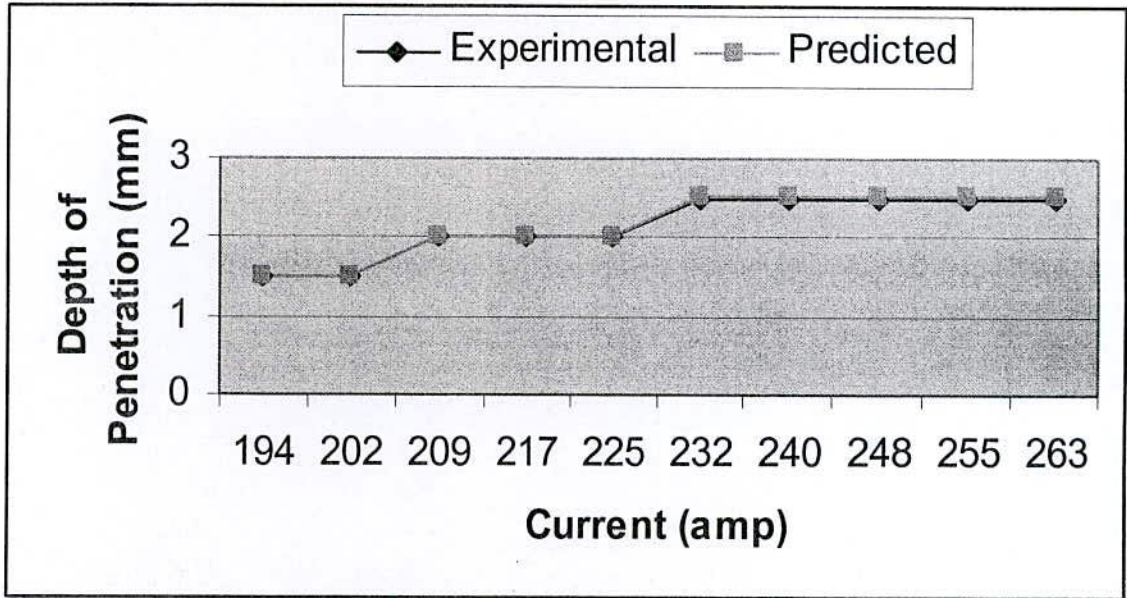


Figure: 5.1 (i) Comparison of Depth of Penetration values using current range from 194 - 263 amps, electrode wire diameter and feed rate respectively 0.8 mm and 4600 mm/min.

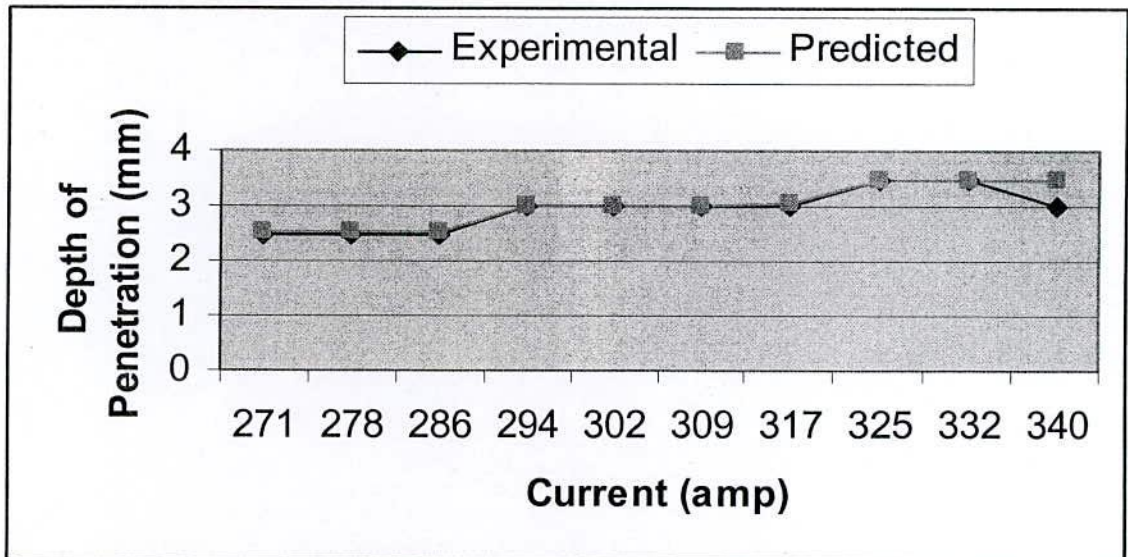


Figure: 5.1 (j) Comparison of Depth of Penetration values using current range from 271 - 340 amps, electrode wire diameter and feed rate respectively 0.8 mm and 5600 mm/min.

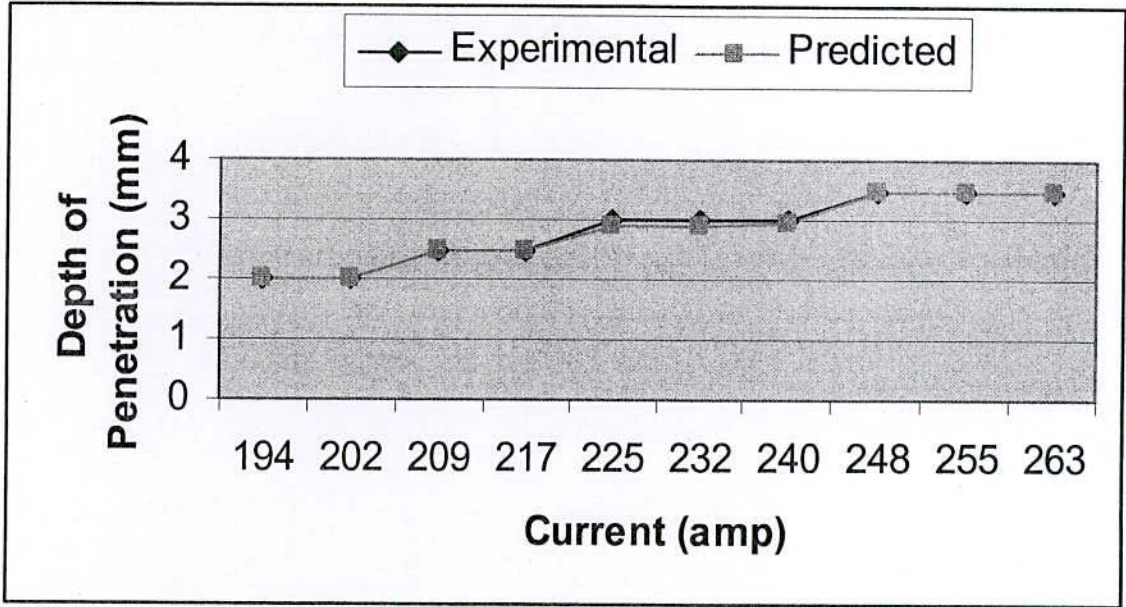


Figure: 5.1 (k) Comparison of Depth of Penetration values using current range from 194 - 263 amps, electrode wire diameter and feed rate respectively 1.0 mm and 4600 mm/min.

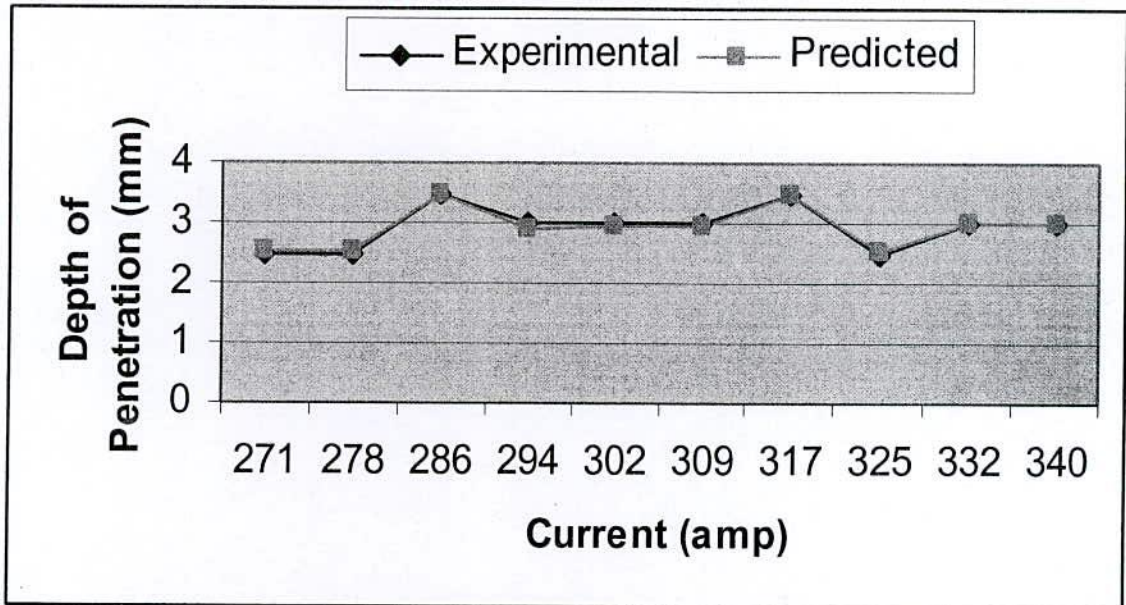


Figure: 5.1 (l) Comparison of Depth of Penetration values using current range from 271 - 340 amps, electrode wire diameter and feed rate respectively 1.0 mm and 5600 mm/min.

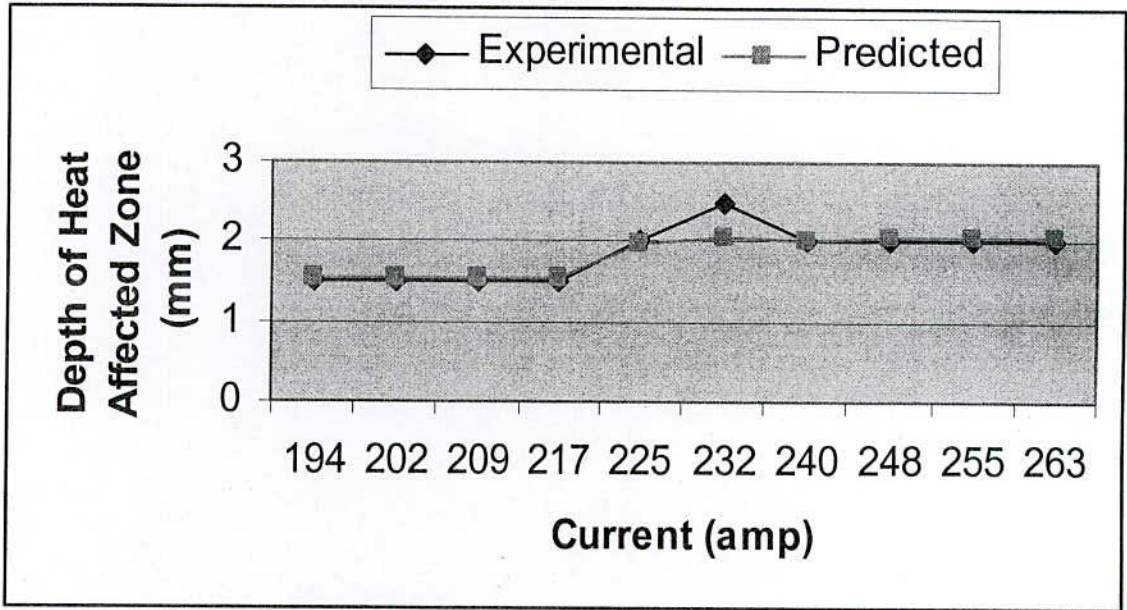


Figure: 5.1 (m) Comparison of Depth of HAZ values using current range from 194 - 263 amps, electrode wire diameter and feed rate respectively 0.8 mm and 4600 mm/min.

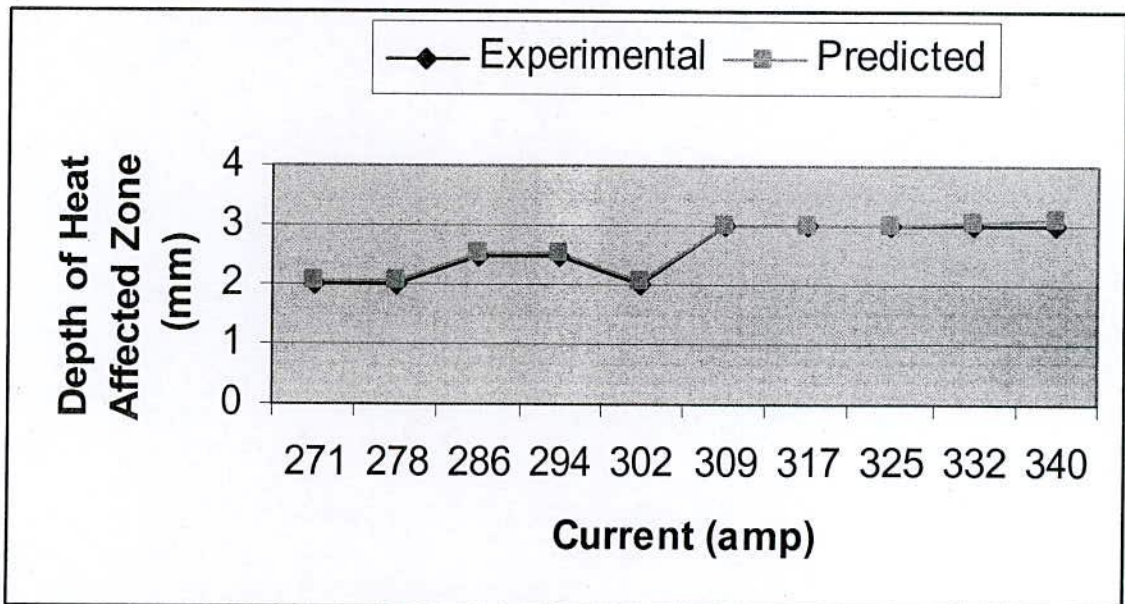


Figure: 5.1 (n) Comparison of Depth of HAZ values using current range from 271 - 340 amps, electrode wire diameter and feed rate respectively 0.8 mm and 5600 mm/min.

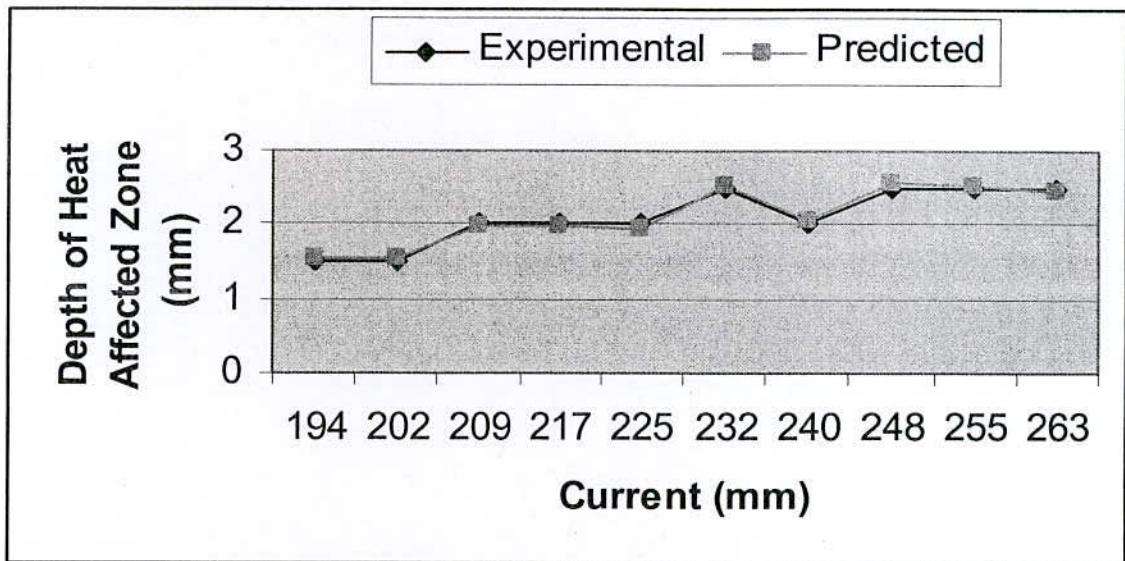


Figure: 5.1 (o) Comparison of Depth of HAZ values using current range from 194 - 263 amps, electrode wire diameter and feed rate respectively 1.0 mm and 4600 mm/min.

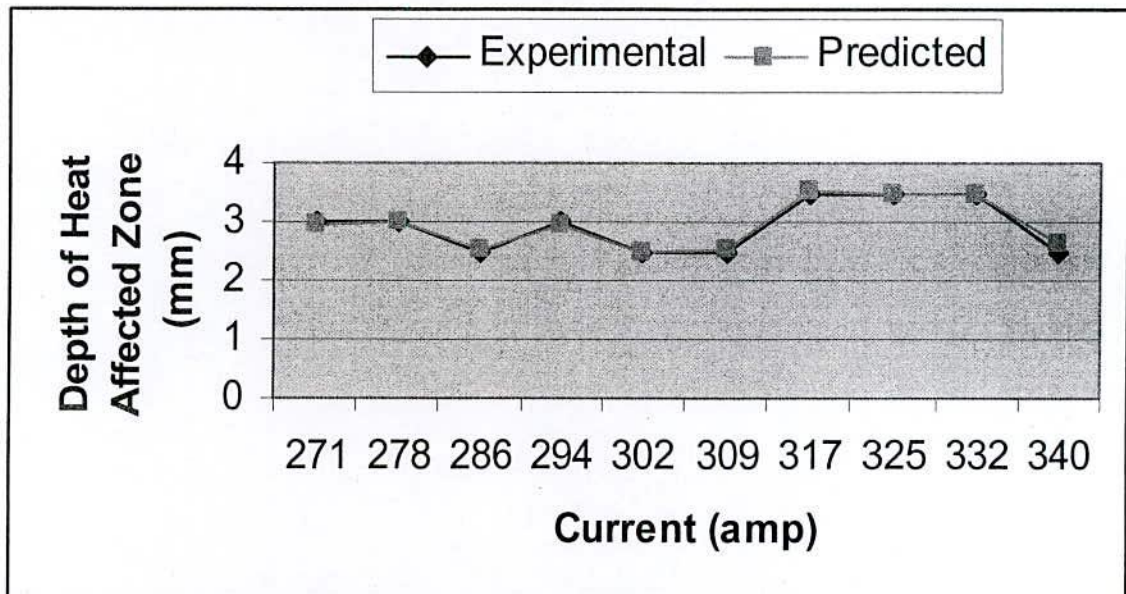


Figure: 5.1 (p) Comparison of Depth of HAZ values using current range from 271 - 340 amps, electrode wire diameter and feed rate respectively 1.0 mm and 5600 mm/min.

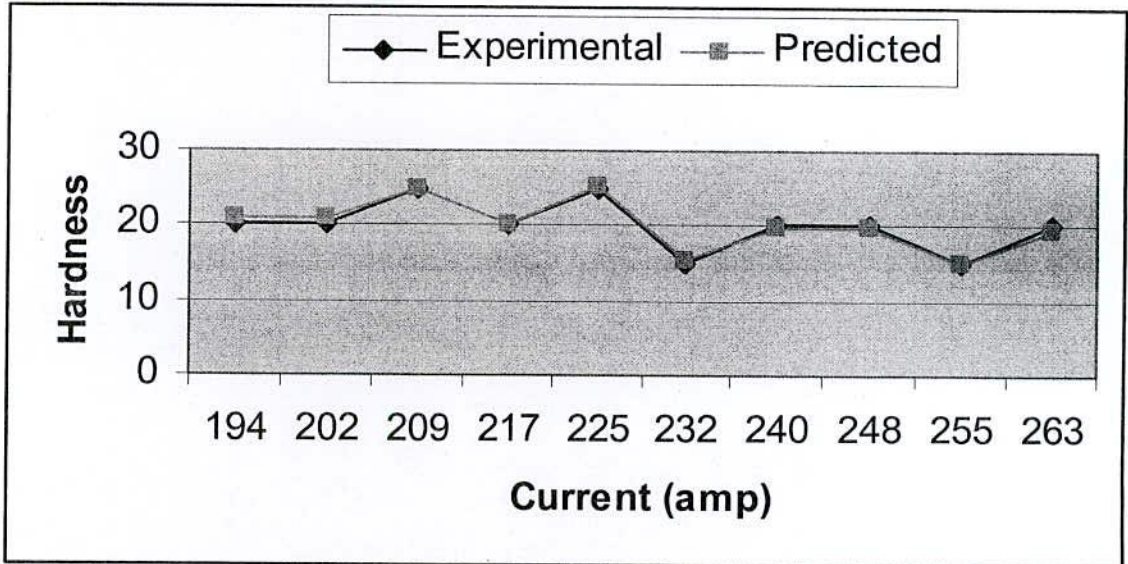


Figure: 5.1 (q) Comparison of Hardness values using current range from 194 - 263 amps, electrode wire diameter and feed rate respectively 0.8 mm and 4600 mm/min.

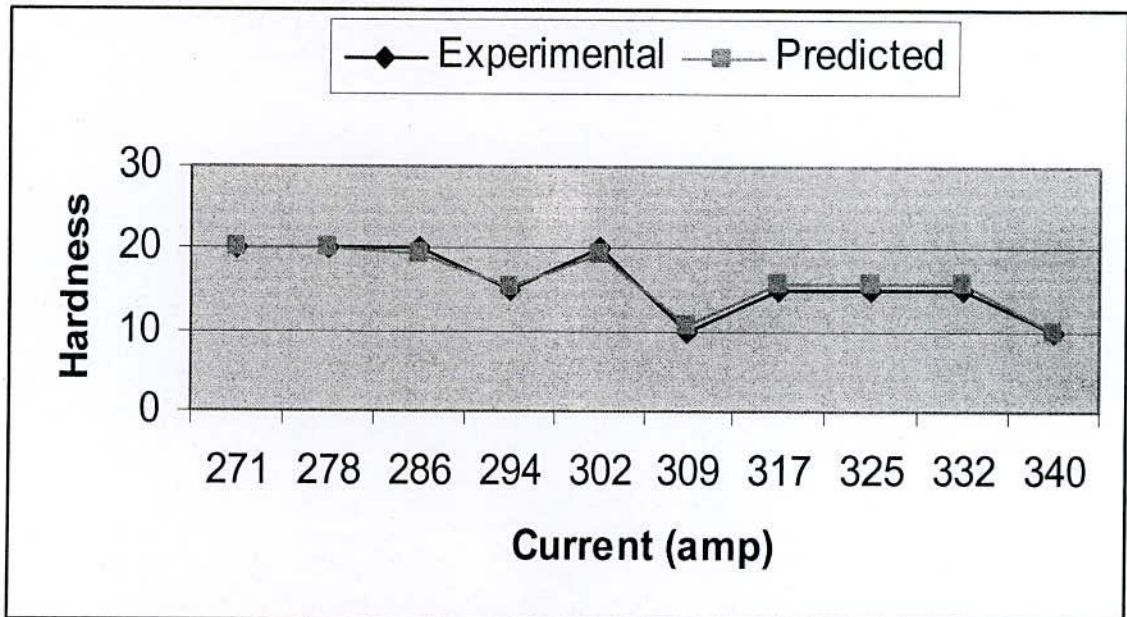


Figure: 5.1 (r) Comparison of Hardness values using current range from 271 - 340 amps, electrode wire diameter and feed rate respectively 0.8 mm and 5600 mm/min.

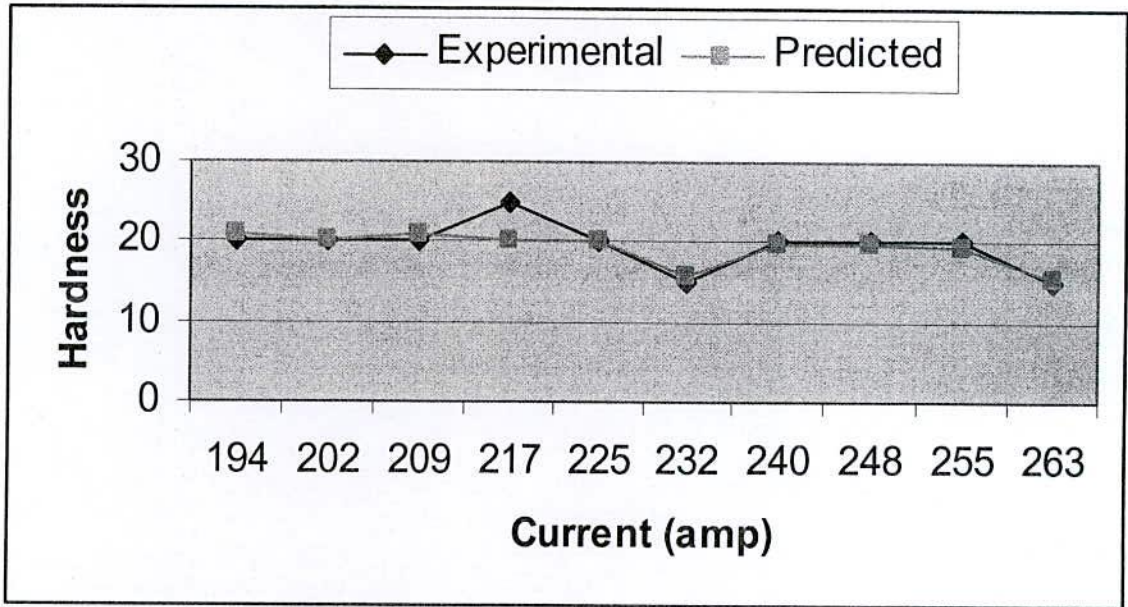


Figure: 5.1 (s) Comparison of Hardness values using current range from 194 - 263 amps, electrode wire diameter and feed rate respectively 1.0 mm and 4600 mm/min.

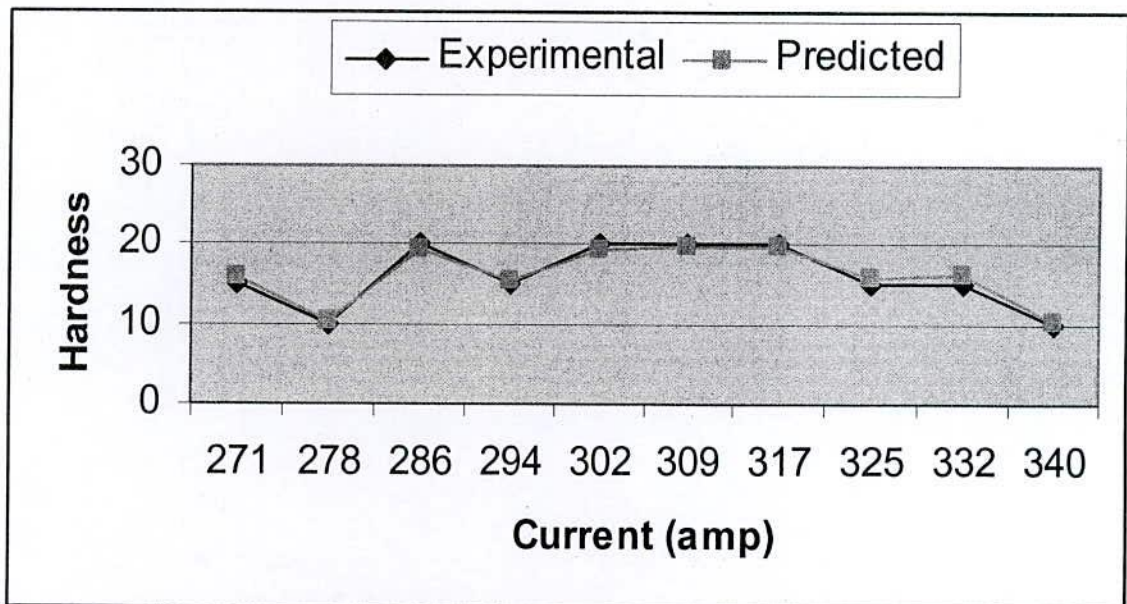


Figure: 5.1 (t) Comparison of Hardness values using current range from 271 - 340 amps, electrode wire diameter and feed rate respectively 1.0 mm and 5600 mm/min.

5.2 Discussions

Some important process parameters, which have intensive effect on weldment characteristics, have not been possible to consider due to the limitations of variable facilities. However, from the figures 5.1 (a) – 5.1 (t) in Art.5.1, the observations have been mentioned in the following sections.

From *Figure: 5.1 (a) – 5.1 (d)* – it has been observed that for both 0.8 & 1.0 mm diameter electrode wire, with increasing the current the bead width increases at both 4600 & 5600 mm/min electrode wire feed rate. And it is very clear that, at maximum welding current, electrode wire diameter and electrode wire feed rate, the bead width is maximum; because the melting rate of electrode wire increases at higher current.

From *Figure: 5.1 (e) – 5.1 (h)* – it has been observed that for 0.8 & 1.0 mm diameter electrode wire there has a little tendency of decreasing in bead height with increasing the current & electrode wire feed rate respectively. But the bead height increases with increasing electrode wire diameter for individual considerations; because at higher current the more molten electrode wire generally minimizes by increasing the bead width, not by bead height.

From *Figure: 5.1 (i) – 5.1 (l)* – it has been observed that for same electrode wire feed rate and within the same welding current range the depth of penetration values have increased with increasing the electrode wire diameter. Again it has also been observed that for same electrode wire diameter the depth of penetration values have increased with increasing the electrode wire feed rate and welding current range simultaneously. Because welding current has great effect on welding temperature which is directly involves melting the electrode wire and base metal as well as electrode wire diameter has played an effective role to maintain the welding zone periphery.

From *Figure: 5.1 (m) – 5.1 (p)* – it has been observed that for same electrode wire feed rate and within the same welding current range the depth of heat affected zone values have

increased with increasing the electrode wire diameter. Again it has also been observed that for same electrode wire diameter the depth of heat affected zone values have increased with increasing the electrode wire feed rate and welding current range simultaneously. Because welding current has great effect on welding temperature which is directly involves melting the electrode wire and base metal as well as electrode wire diameter has played an effective role to maintain the welding zone periphery. However, there has observed a little bit exceptions have occurred on depth of heat affected zone values, probably due to the lack of stability of involved parameters.

From *Table & Figure: 5.1 (q) – 5.1 (t)* – it has been observed that for same electrode wire feed rate and within the same welding current range the hardness values have found more or less steady for an individual electrode wire diameter. Again for an individual electrode wire diameter the hardness values have found in decreasing manner with increasing the electrode wire feed rate and welding current range simultaneously. Because up to a moderate range of welding temperature and at higher welding temperature, where welding temperature is directly proportional to the welding current, the formation of molecular structure of penetrated zone are different, so different hardness have found.

In all the cases the experimental values and the computational values have found to be very close, indicating that the computational values are quite dependable to be used for prediction.

5.2.1 Correlation

As mentioned in a published paper “*Modeling and predicting the effects of process parameters on weldment characteristics in shielded metal arc welding* by M. M. Mahapatra, M. Sadat Ali, G. L. Dutta and B. Pradhan in *Indian Welding Journal*, 38(2), 2005, pp.22-29”; a few important results in graphical form have been copied in the following sections, which are almost identical with the results of this research works illustrated in Art. 5.1.3 and described in Art. 5.2. Although welding process in one is *SMA welding* and in another is *MIG welding*.

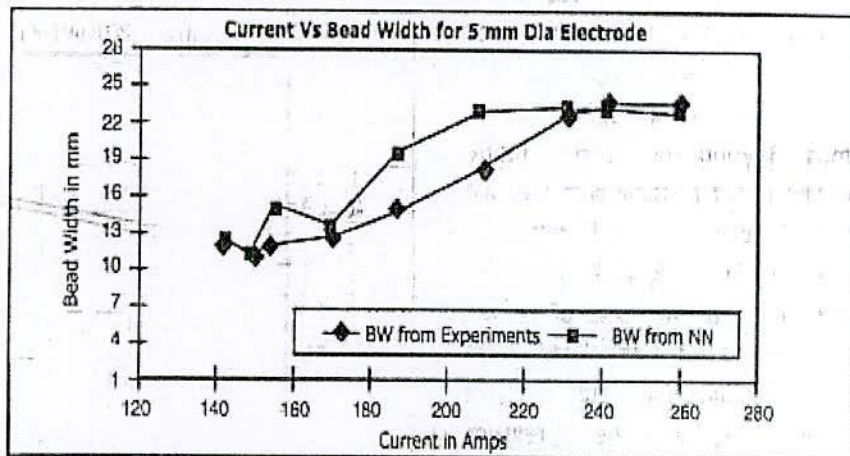


Figure 5.1(a): Current vs Bead Width for 5 mm Diameter Electrode.

The above figure exhibits the same trends of bead width characteristics as illustrated in Figure: 5.1(a) – 5.1(d).

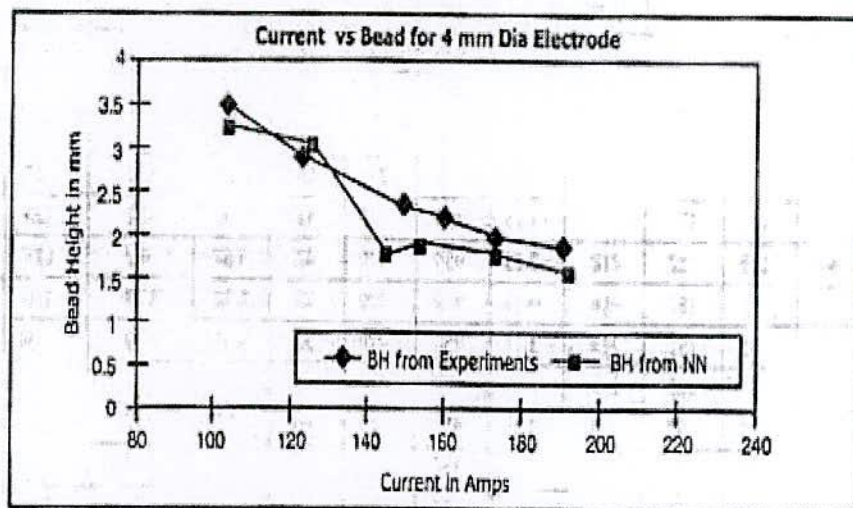


Figure 5.1(e): Current vs Bead Height for 4 mm Diameter Electrode

The above figure exhibits the same trends of bead height characteristics as illustrated in Figure: 5.1(e) – 5.1(h).

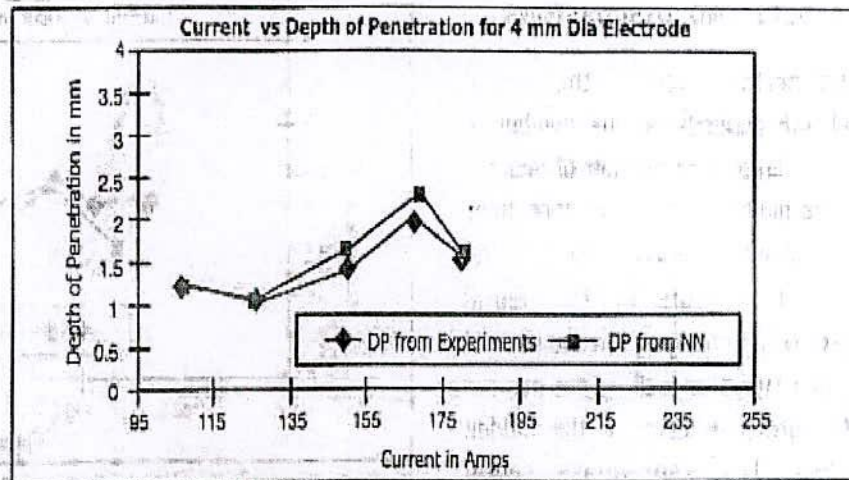


Figure : Current vs Depth of Penetration for 4mm Diameter Electrode

The above figure exhibits the same trends of depth of penetration characteristics as illustrated in *Figure: 5.1(i) – 5.1(l)*.

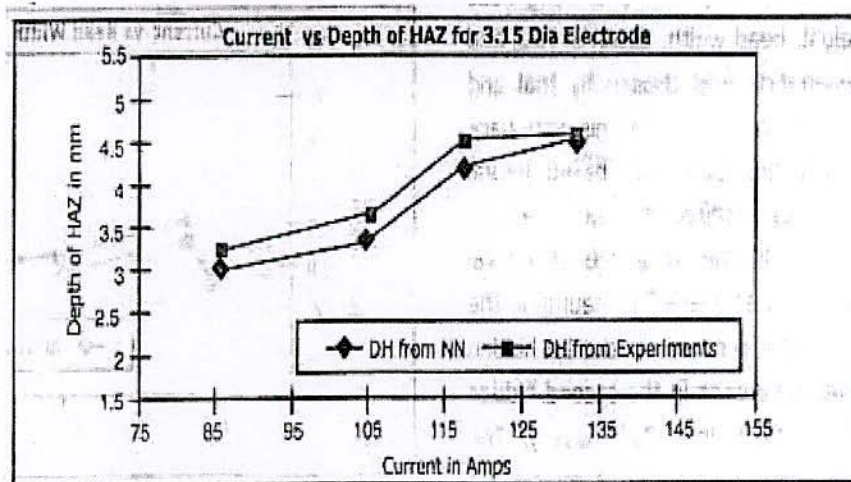


Figure Current vs depth of HAZ for 3.15 mm Diameter Electrode

The above figure exhibits the same trends of depth of HAZ characteristics as illustrated in *Figure: 5.1(m) – 5.1(p)*.

CONCLUSIONS AND RECOMMENDATIONS

6.1 Conclusions

1. Artificial neural networks based approaches can be used effectively for predicting the output parameters like bead width, bead height, depth of penetration, depth of HAZ and hardness.
2. The effects of the welding process parameters on weldment characteristics can be summarized in the following way:
 - a) Welding current, electrode wire diameter, electrode wire feed rate appear to be important process parameters in MIG welding, with their direct effects on bead geometry shape, size, depth of penetration and HAZ also.
 - b) With increase in the current and wire diameter, the bead width increase moderately linearly. There has no considerable effect of changing the wire feed rate.
 - c) With increasing the current and wire feed rate there has no notable change in the bead height, but increase with increasing the wire diameter.
 - d) With increasing the current for an electrode wire diameter and an electrode wire feed rate, the depth of penetration increases.
 - e) Change in process parameters exhibits effect on depth of HAZ in same manner as for depth of penetration.

- f) For every change in process parameters during the experiment shows a significant change in hardness. With hardness of base metal having average value of 5, after welding these appears as much as in the range of 10 to 20.

6.2 Recommendations

1. The experiment can be done using more number of important process parameters variables which has not been used in this experiment due to some limitations. This will result more accurate predictions of the weldment characteristics.
2. This method can be applied to other welding processes like TIG (Tungsten Inert Gas) welding, SAW (Submerged Arc Welding) etc. using semi-automatic and automatic processes.

REFERENCES

1. Khanna O. P., *A text book of Welding Technology*, Dhanpat Rai Publications (P) Ltd., New Delhi, (2003), pp. 1 – 8, 80 – 87.
2. Mahapatra M. M., Sadat Ali M., Datta G. L. and Pradhan B., *Modeling and Predicting the effects of process parameters on weldment characteristics in shielded metal arc welding*, Indian Welding Journal, 38(2), 2005, pp. 22 – 29.
3. Nagesh D. S. and Datta G. L., *Prediction of weld bead geometry and penetration in shielded metal arc welding using artificial neural networks*, Journal of Material Processing Technology, 123(2), 2002, pp. 303 – 312.
4. Faruk A. A., Hasib M. A., Ahmed M. N., and Das U. K., *Prediction of Weld Bead Geometry and Penetration in Electric Arc Welding using Artificial Neural Networks*, International Journal of Mechanical & Mechatronics Engineering IJMME-IJENS, 10(4), 2008, pp. 23 – 28.
5. Kim I. S., Son J. S., Park C. E., Kim I. J. and Kim H. H., *An investigation into an intelligent system for predicting bead geometry in GMA welding process*, Journal of Material Processing Technology, 159, 2005, pp. 113 – 118.
6. Dey V., Pratihar D.K. and Datta, G.L., *Prediction of Weld Bead Profile Using Neural Networks*, proceedings of the 1ST International Conference, ICETET'08 on Emerging Trends in Engineering and Technology, (on page(s): 581 - 586), held on 16 – 18 July, 2008 at Nagpur, Maharashtra, India.
7. Srihari T. and Parmar R. S., *Weld bead geometry prediction*, Journal of The Institution of Engineers (India), Mechanical Engineering Division, 76, 1995, pp. 39 – 43.

8. Murugan N. and Parmar R. S., *Effects of MIG process parameters on the geometry of the bead in the automatic surfacing of stainless steel*, Journal of Materials Processing Technology, 41(4), 1994, pp. 381 – 398.
9. Hyeong-Soon Moon and Suck-Joo Na, *Optimum design based on mathematical model and neural network to predict weld parameters for fillet joints*, Journal of Manufacturing Systems, 16(1), 1997, pp. 13 – 23.
10. Nagesh D. S. and Datta G. L., *Genetic algorithm for optimization of welding variables for height to width ratio and application of ANN for prediction of bead geometry for TIG welding process*, Journal of Applied Soft Computing, 10(3), 2010, pp. 897 – 907.
11. Murugan N. and Gunaraj V., *Prediction and control of weld bead geometry and shape relationships in submerged arc welding of pipes*, Journal of Materials Processing Technology, 168(3), 2005, pp. 478 – 487.
12. Erdal Karadeniza, Ugur Ozsaracb and Ceyhan Yildizc, *The effect of process parameters on penetration in gas metal arc welding processes*, Journal of Materials and Design, 28(2), 2007, pp. 649 – 656.
13. Benyounisa K. Y., and Olabib A. G., *Optimization of different welding processes using statistical and numerical approaches – A reference guide*, Journal of Advances in Engineering Software, 39(6), 2008, pp. 483 – 496.
14. Simon Haykin, *Neural Networks, A Comprehensive Foundation*, 2nd edition, 2001, pp. 1 – 63, 756 – 761.

Appendix – 1

Specifications and Calibrations of used all machines & equipments

Vernier Slide Caliper	:	Company	: MAUSER
		Brand	: INOX
		Range	: 0 – 25 cm
		Calibration	: 1 mm
		Accuracy	: 0.01 mm
		(Linearity and Accuracy is satisfactory)	
MIG Welding Machine	:	Company:	ESAB Welding Equipment AB (Sweden) Murex Welding Products Ltd. (England)
		Model	: Transmig 350C (Semi-automatic)
		Input Voltage:	400 – 415 V, 3 ~ 50/60 Hz
		Setting Range (DC):	40A/16V – 340A/31V
		Open Circuit Voltage:	16 – 40 V
		Open Circuit Power:	240 W
		Efficiency:	77 %
		Wire Feed Speed:	1.9 – 20 m/min
		Duty cycle:	30, 60 & 100 %
		Welding Gun Connection:	EURO
		Operating Temperature:	-10 to +40 ⁰ C
		Enclosure class:	IP23
		Application class:	S
Rock Well Hardness Testing Machine	:	Company	: HOYTOM Ltd. (Spain)
		Model	: 1003 A
		Loading Capacity	: 31.25 – 187.5 kg
		Dial Calibration	: B & C scale 0 – 100 (Unique division)

Appendix – 2

Program on Real-Time Recurrent Learning Algorithm

```
/* Real Time Recurrent learning for flux estimation
Page 756, Book: SIMON HAYKEN
NO Hidden layer
Rewrite in New form that is one weight matrix (wa21) */

#include <stdio.h>
#include <math.h>
#include <stdlib.h>
#include <string.h>
#include <time.h>

#define IN 4
#define STATE 5
#define OUT 5
#define MPN 40
#define constant 0.06
//define f1(x) (1.0-exp(-2.0*x))/(1.0+exp(-2.0*x))
#define f1(x) 1.0/(1.0+exp(-2.0*x))
//define f1(x) (constant*x)
#define rnd() (((float)rand()/0x7fff)*(Wmax-Wmin)+Wmin)

float state_pre[MPN][STATE];
float state_pre_pre[MPN][STATE];
float state_pre_pre_pre[MPN][STATE];
float state_pre_pre_pre_pre[MPN][STATE];
float input[MPN][IN];
float U[STATE][STATE+IN];
float u[MPN][OUT];
float wa21[STATE][STATE+IN];
float dwa21[STATE][STATE+IN];
float diagonal [STATE][STATE];
float output[MPN][STATE];
float output_pre[MPN][STATE];
float target[MPN][OUT];
float partial_derivative[STATE][STATE+IN];
float partial_derivative_pre[STATE][STATE+IN ];
float ef;
float ef1[OUT];
float ef2[MPN][OUT];
//float beta=0.000000008;//current
//float beta=0.00000001;//sarwer
//float alpha=0.0000001;
```




```

float beta=0.000000008;
float alpha=0.0000000025;
//float alpha=0.0;
float Wmax=0.0001;
float Wmin=-0.0001;

int tm;

FILE *fps,*fps1,*fps3;

main ()
{
    int i, j, k;
    void propagation(int p);
        void back_propagation(int p);
        void read_file();
        void readmth();
    read_file();
    readmth();

    /*----- Before Learning ----- */

        for( j=0; j < MPN; j++) {
            propagation(j);
                for( k=0; k < OUT; k++) {
                    ef2[j][k]=0.0;
                    ef2[j][k] += u[j][k]-target[j][k];
                }
            }
        for( k=0; k < OUT; k++) {
            ef1[k]=0.0;
            for( j=0; j < MPN; j++) {
                ef1[k]+=ef2[j][k]*ef2[j][k];
            }
            ef1[k]=sqrt(ef1[k])/MPN;
        }
        for(ef=0.0, k=0; k < OUT ; k++) {
            ef+=ef1[k]*ef1[k];
        }
        ef=sqrt(ef)/OUT;

    tm=0;
    fps3=fopen("error.dat","w");
    fps=fopen("result.dat","w");
    fps1=fopen("weight.dat","w");
    // fps3=fopen("error_filter_a.dat","w");

```

```

//fps=fopen("result_filter_a.dat","w");
//fps1=fopen("weight1_filter_a.dat","w");

printf("%10f %d\n", ef, tm);

/* ----- Start to learn ----- */

//for( tm=1; ef>0.0000796; tm++) {
for( tm=1; ef>0.006061; tm++) {
    for(j=0; j < MPN; j++) {
        propagation(j);
        back_propagation(j);
    }
    for( j=0; j < MPN; j++) {
        propagation(j);
        for( k=0; k < OUT; k++) {
            ef2[j][k]=0.0;
            ef2[j][k] += u[j][k]-target[j][k];
        }
        for( k=0; k < OUT; k++) {
            ef1[k]=0.0;
            for( j=0; j < MPN; j++) {
                ef1[k]+=ef2[j][k]*ef2[j][k];
            }
            ef1[k]=sqrt(ef1[k])/MPN;
        }
        for(ef=0.0, k=0; k < OUT ; k++) {
            ef+=ef1[k]*ef1[k];
        }
        ef=sqrt(ef)/OUT;
/* for(i=0; i < STATE; i++){
for(j=0; j < STATE; j++){

    fprintf(fps3,"%f ",wa21[i][j]);
        }
    }
    fprintf(fps3,"\n ");*/
        if(tm% 1000==0){
            printf("%.10f %d \n", ef, tm);
            fprintf(fps3," %d %.10f\n", tm, ef);
            //printf("%.10f %d %.10f %.10f\n", ef,
tm,u[500][1],target[500][1]);
            //fprintf(fps3,"%10f %d %.10f %.10f\n", ef, tm,u[500][1],target[500][1]);
        }
    }
}

```

```

printf("%.6f %d\n",ef,tm);
fprintf(fps, "%.6f %d\n",ef,tm);

/* ----- learning over-saving weights & printing output ----- */
// fprintf(fps2, "\nweight between state & hidden neuron\n");

    for(i=0; i < STATE; i++) {
        for(j=0; j < STATE+IN; j++){

fprintf(fps1, "%f ", wa21[i][j]);
fprintf(fps1, "\n");
        }
    }

    for(i=0; i < MPN; i++) {

    fprintf(fps, "\t %.6f  %.6f %.6f  %.6f %.6f  %.6f %.6f  %.6f %.6f  %.6f",
target[i][0],u[i][0], target[i][1],u[i][1],target[i][2],u[i][2],
target[i][3],u[i][3],target[i][4],u[i][4]);
        fprintf(fps, "\n");
    }
    fclose(fps);
}

/* ----- close main ----- */

void propagation(int p)
{
    int i,j,k,l;
    float net,net1,sum[STATE];
    for(net=0.0,net1=0.0, i=0; i < STATE; i++){
state_pre_pre_pre_pre[p][i]=state_pre_pre_pre[p][i];
state_pre_pre_pre[p][i]=state_pre_pre[p][i];
state_pre_pre[p][i]=state_pre[p][i];
state_pre[p][i]=output[p][i];
//input[p][IN-1]=state_pre_pre[p][i];
//input[p][IN-2]=state_pre_pre_pre[p][i];
//input[p][IN-3]=state_pre_pre_pre_pre[p][i];
for(j=0; j < STATE; j++){
net+=wa21[i][j]*state_pre[p][j];
}
for(k=0; k < IN; k++){
net1+=wa21[i][STATE+k]*input[p][k];
}
sum[i]=net+net1;
output[p][i]=f1(sum[i]);
}

```

```

    }
    for( l=0; l < OUT; l++){
        //target[p][l]=state_pre[p][l];
        target[p][l]=output[p][l];
    }
}
void back_propagation(int p)
{
    int i,j,k;
    float sum3[STATE][STATE+IN],sum4[STATE][STATE+IN];
    for(i=0; i < STATE; i++){
        for(k=0; k < STATE+IN; k++){
            sum3[i][k]=0.0;
            for(j=0; j < STATE; j++){
                partial_derivative_pre[j][k]=partial_derivative[j][k];
                sum3[i][k]+=wa21[i][j]*partial_derivative_pre[j][k];
            }
        }
    }

    for(j=0; j < STATE; j++){
        for(k=0; k < STATE; k++){
            U[j][k]=state_pre[p][k];
        }
        for(i=0; i < IN; i++){
            U[j][i+STATE]=input[p][i];
        }
    }

    for(j=0; j < STATE; j++){
        for(k=0; k < STATE+IN; k++){
            sum4[j][k]= sum3[j][k]+U[j][k];
        }
    }

    for(i=0; i < STATE; i++){
        for(j=0; j < STATE; j++){
            diagonal[i][j]=0.0;
        }
        //diagonal[i][i]=(1.0+output[p][i])*(1.0-output[p][i]);
        diagonal[i][i]=output[p][i]*(1.0-output[p][i]);
        //diagonal[i][i]=constant;
    }
    for(i=0; i < STATE; i++){
        for(k=0; k < STATE+IN; k++){

```

```

partial_derivative[i][k]=0.0;
for(j=0; j < STATE; j++){

    partial_derivative[i][k]+=diagonal[i][j]*sum4[j][k];
    }
}

for(i=0; i < STATE; i++){
    for(j=0; j < STATE+IN; j++){
dwa21[i][j]=beta*partial_derivative_pre[i][j]*ef2[p][i];
wa21[i][j]+=dwa21[i][j]+alpha*dwa21[i][j];
    }

}

/* wa21[0][2]=0.0;
wa21[0][3]=0.0;
wa21[0][4]=0.0;
wa21[0][5]=0.0;
wa21[0][6]=0.0;*/
//wa21[0][7]=0.0;
// wa21[1][0]=0.0;
}

void read_file()
{
int i,j;
float x;
FILE *fp;
if(( fp=fopen("train1.dat", "r"))==NULL) {
//if(( fp=fopen("field_wsla.dat", "r"))==NULL) {
//if(( fp=fopen("filter_a.dat", "r"))==NULL) {
// if(( fp=fopen("high.dat", "r"))==NULL) {
    }

for(i=0; i < MPN; i++) {
    for(j=0; j < IN; j++){
        fscanf(fp,"%f",&x);
        input[i][j]=x;
    }

    for(j=0; j < OUT; j++){
        fscanf(fp,"%f",&x);
        u[i][j]=x;
    }
}
}

```

```

fclose(fp);
    }

    void readmth()
    {
        int i,j;
        float y;
        FILE *fp1;
        //if(( fp1=fopen("weight_dfr2.dat", "r"))==NULL) {}
        for(i=0; i < STATE; i++) {
            for(j=0; j < STATE+IN; j++){
                wa21[i][j] = rnd();
                dwa21[i][j] = 0.0;
                //fscanf(fp1, "%f", &y);
                //wa21[i][j]=y;
            }
        }
    }
}

```

Appendix – 3
Mathematical Model

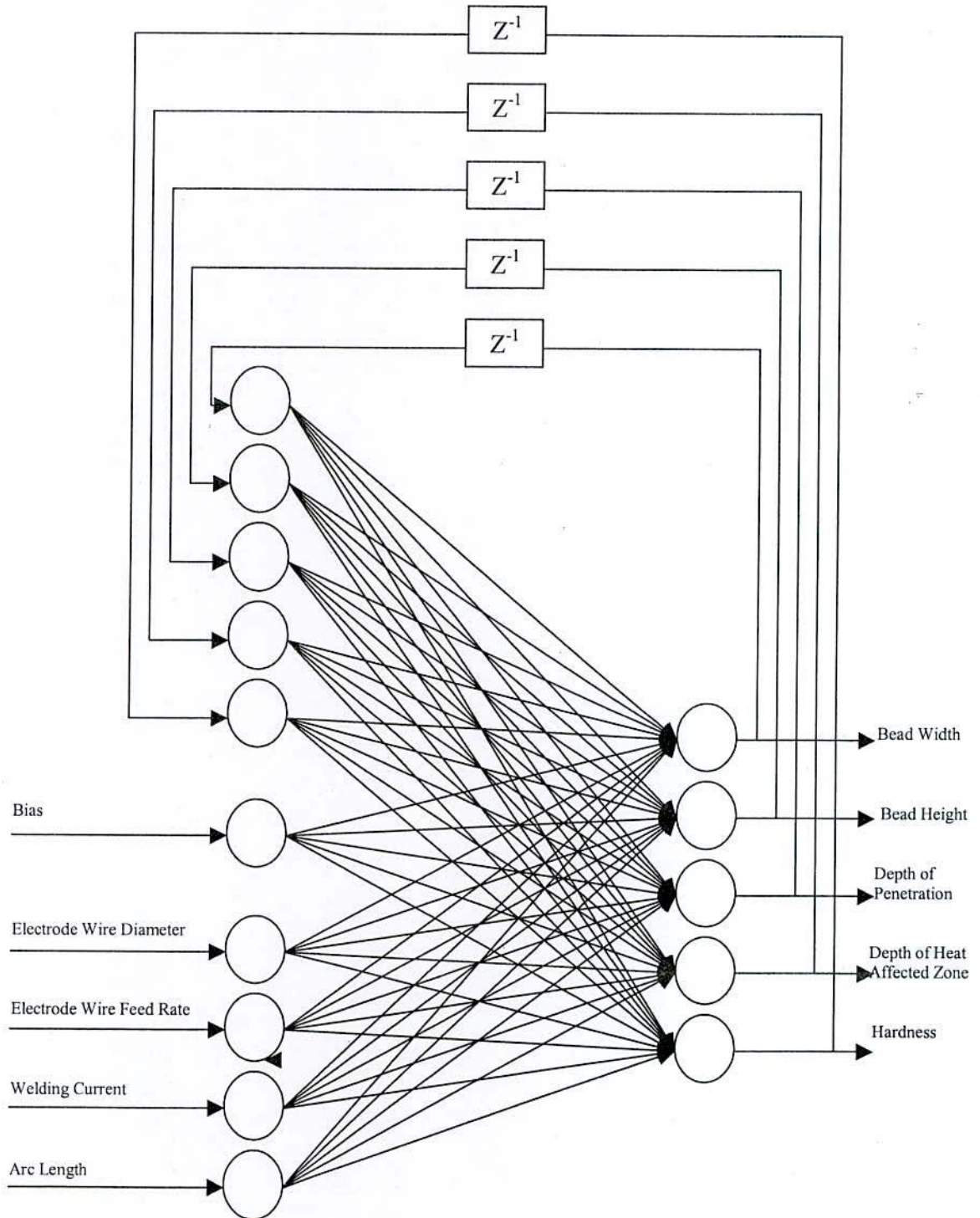


Figure: A3.1 Block diagram of network

It can be derived the Eqs. 3.5.1, 3.5.2 and latter on of Art. 3.5 in CHAPTER 3 by replacing the values of m, p, q, weight vectors and functions. Where, m = dimensionality of input space = 4, p = dimensionality of output space = 5, q = dimensionality of state space = 5. In input space, there has a bias, which is dependent on state space dimensionality. By following these, the state space model of the network can be rewrite as the following matrix form.

$$x_1(n+1) = \varphi (Wa_{11}x_1(n) + \dots + Wa_{15}x_5(n) + Wb_{11}u_1(n) + \dots + Wb_{14}u_4(n) + Wb_{15}*1)$$

$$x_2(n+1) = \varphi (Wa_{21}x_1(n) + \dots + Wa_{25}x_5(n) + Wb_{21}u_1(n) + \dots + Wb_{24}u_4(n) + Wb_{25}*1)$$

$$x_3(n+1) = \varphi (Wa_{31}x_1(n) + \dots + Wa_{35}x_5(n) + Wb_{31}u_1(n) + \dots + Wb_{34}u_4(n) + Wb_{35}*1)$$

$$x_4(n+1) = \varphi (Wa_{41}x_1(n) + \dots + Wa_{45}x_5(n) + Wb_{41}u_1(n) + \dots + Wb_{44}u_4(n) + Wb_{45}*1)$$

$$x_5(n+1) = \varphi (Wa_{51}x_1(n) + \dots + Wa_{55}x_5(n) + Wb_{51}u_1(n) + \dots + Wb_{54}u_4(n) + Wb_{55}*1)$$

and

$$y_1(n) = Cx_1(n)$$

$$y_2(n) = Cx_2(n)$$

$$y_3(n) = Cx_3(n)$$

$$y_4(n) = Cx_4(n)$$

$$y_5(n) = Cx_5(n)$$

and

$$Wa = \begin{bmatrix} Wa_{11} & Wa_{12} & Wa_{13} & Wa_{14} & Wa_{15} \\ Wa_{21} & Wa_{22} & Wa_{23} & Wa_{24} & Wa_{25} \\ Wa_{31} & Wa_{32} & Wa_{33} & Wa_{34} & Wa_{35} \\ Wa_{41} & Wa_{42} & Wa_{43} & Wa_{44} & Wa_{45} \\ Wa_{51} & Wa_{52} & Wa_{53} & Wa_{54} & Wa_{55} \end{bmatrix}$$

and

$$Wb = \begin{bmatrix} Wb_{11} & Wb_{12} & Wb_{13} & Wb_{14} & Wb_{15} \\ Wb_{21} & Wb_{22} & Wb_{23} & Wb_{24} & Wb_{25} \\ Wb_{31} & Wb_{32} & Wb_{33} & Wb_{34} & Wb_{35} \\ Wb_{41} & Wb_{42} & Wb_{43} & Wb_{44} & Wb_{45} \\ Wb_{51} & Wb_{52} & Wb_{53} & Wb_{54} & Wb_{55} \end{bmatrix}$$

and

$$C = \begin{bmatrix} 1 & 0 & 0 & 0 & 0 \\ 0 & 1 & 0 & 0 & 0 \\ 0 & 0 & 1 & 0 & 0 \\ 0 & 0 & 0 & 1 & 0 \\ 0 & 0 & 0 & 0 & 1 \end{bmatrix}$$

Appendix – 4

Comparison of experimental and computational values of different weldment characteristics in tabular form with percentage of error

Table: A4.1 Bead Width

Process Parameters			Bead Width Values		Percentage of Error
Wire Dias (mm)	Wire feed rate (mm/min)	Welding current (amp)	Experimental (mm)	Computational (mm)	
0.8	4600	194	7.00	7.0251	0.3586
0.8	4600	202	7.00	7.0369	0.5271
0.8	4600	209	7.50	7.5288	0.3840
0.8	4600	217	7.50	7.5327	0.4360
0.8	4600	225	8.00	8.0423	0.5288
0.8	4600	232	8.50	8.5478	0.5624
0.8	4600	240	9.00	9.0492	0.5467
0.8	4600	248	9.50	9.5287	0.3021
0.8	4600	255	10.00	10.0639	0.6390
0.8	4600	263	10.00	10.0471	0.7410

Table: A4.2 Bead Width

Process Parameters			Bead Width Values		Percentage of Error
Wire Dias (mm)	Wire feed rate (mm/min)	Welding current (amp)	Experimental (mm)	Computational (mm)	
0.8	5600	271	11.00	11.0729	0.6627
0.8	5600	278	11.00	11.0467	0.4245
0.8	5600	286	11.00	11.0821	0.7464
0.8	5600	294	11.50	11.5934	0.8122
0.8	5600	302	11.50	11.5626	0.5443
0.8	5600	309	12.00	12.0345	0.2875
0.8	5600	317	12.50	12.5573	0.4584
0.8	5600	325	12.50	12.5828	0.6624
0.8	5600	332	13.00	13.0652	0.5015
0.8	5600	340	13.00	13.0981	0.7546

Table: A4.3 Bead Width

Process Parameters			Bead Width Values		Percentage of Error
Wire Dias (mm)	Wire feed rate (mm/min)	Welding current (amp)	Experimental (mm)	Computational (mm)	
1.0	4600	194	8.00	8.0326	0.4075
1.0	4600	202	8.00	8.0434	0.5425
1.0	4600	209	10.00	9.9424	0.5760
1.0	4600	217	10.00	9.9365	0.6350
1.0	4600	225	11.00	10.9572	0.3891
1.0	4600	232	12.50	12.4358	0.5136
1.0	4600	240	12.50	12.4208	0.6336
1.0	4600	248	12.50	12.4455	0.4360
1.0	4600	255	13.50	13.4217	0.5800
1.0	4600	263	13.50	13.3854	0.8489

Table: A4.4 Bead Width



Process Parameters			Bead Width Values		Percentage of Error
Wire Dias (mm)	Wire feed rate (mm/min)	Welding current (amp)	Experimental (mm)	Computational (mm)	
1.0	5600	271	14.00	13.9257	0.5307
1.0	5600	278	14.50	14.4308	0.4772
1.0	5600	286	15.00	14.9165	0.5567
1.0	5600	294	15.00	14.9202	0.5320
1.0	5600	302	15.00	14.8705	0.8633
1.0	5600	309	15.50	15.4726	0.1768
1.0	5600	317	15.50	15.3872	0.7277
1.0	5600	325	16.00	15.9217	0.4894
1.0	5600	332	16.00	15.9183	0.5106
1.0	5600	340	16.00	15.8924	0.6725

Table: A4.5 Bead Height

Process Parameters			Bead Height Values		Percentage of Error
Wire Dias (mm)	Wire feed rate (mm/min)	Welding current (amp)	Experimental (mm)	Computational (mm)	
0.8	4600	194	3.50	3.5782	2.2343
0.8	4600	202	3.50	3.5693	1.9800
0.8	4600	209	3.50	3.5328	0.9371
0.8	4600	217	3.50	3.5125	0.3571
0.8	4600	225	3.50	3.5122	0.3486
0.8	4600	232	3.50	3.5113	0.3229
0.8	4600	240	3.50	3.5087	0.2486
0.8	4600	248	3.00	3.0763	2.5433
0.8	4600	255	3.00	3.0385	1.2833
0.8	4600	263	3.00	3.0238	0.7933

Table: A4.6 Bead Height

Process Parameters			Bead Height Values		Percentage of Error
Wire Dias (mm)	Wire feed rate (mm/min)	Welding current (amp)	Experimental (mm)	Computational (mm)	
0.8	5600	271	3.50	3.5293	0.8337
0.8	5600	278	3.50	3.5182	0.5200
0.8	5600	286	3.50	3.4751	0.7114
0.8	5600	294	3.00	3.0187	0.6233
0.8	5600	302	3.00	3.0152	0.5067
0.8	5600	309	3.00	3.0129	0.4300
0.8	5600	317	3.00	3.0151	0.5033
0.8	5600	325	3.00	2.9864	0.4533
0.8	5600	332	3.00	2.9752	0.8267
0.8	5600	340	3.00	2.9678	1.0733

Table: A4.7 Bead Height

Process Parameters			Bead Height Values		Percentage of Error
Wire Dias (mm)	Wire feed rate (mm/min)	Welding current (amp)	Experimental (mm)	Computational (mm)	
1.0	4600	194	4.00	4.0127	0.3175
1.0	4600	202	4.00	4.0495	1.2375
1.0	4600	209	4.00	3.9765	0.5775
1.0	4600	217	4.00	3.9537	1.1575
1.0	4600	225	4.00	3.9821	0.4475
1.0	4600	232	4.50	4.4983	0.0378
1.0	4600	240	4.50	4.4897	0.2289
1.0	4600	248	4.00	3.9873	0.3175
1.0	4600	255	3.50	3.4827	0.4943
1.0	4600	263	3.50	3.4801	0.5686

Table: A4.8 Bead Height

Process Parameters			Bead Height Values		Percentage of Error
Wire Dias (mm)	Wire feed rate (mm/min)	Welding current (amp)	Experimental (mm)	Computational (mm)	
1.0	5600	271	4.00	3.9835	0.4125
1.0	5600	278	4.00	3.9723	0.6925
1.0	5600	286	4.00	3.9687	0.7825
1.0	5600	294	3.00	3.0185	0.6167
1.0	5600	302	3.50	3.5297	0.8486
1.0	5600	309	3.00	3.0141	0.4700
1.0	5600	317	3.00	3.0178	0.5933
1.0	5600	325	3.00	2.9873	0.4233
1.0	5600	332	3.00	2.9756	0.8133
1.0	5600	340	2.50	2.5274	0.9880

Table: A4.9 Depth of Penetration

Process Parameters			Depth of Penetration Values		Percentage of Error
Wire Dias (mm)	Wire feed rate (mm/min)	Welding current (amp)	Experimental (mm)	Computational (mm)	
0.8	4600	194	1.50	1.5156	1.0400
0.8	4600	202	1.50	1.5149	0.9933
0.8	4600	209	2.00	2.0243	1.2150
0.8	4600	217	2.00	2.0251	1.2550
0.8	4600	225	2.00	2.0235	1.1750
0.8	4600	232	2.50	2.5109	0.4360
0.8	4600	240	2.50	2.5207	0.8280
0.8	4600	248	2.50	2.5225	0.9000
0.8	4600	255	2.50	2.5233	0.9320
0.8	4600	263	2.50	2.5247	0.9880

Table: A4.10 Depth of Penetration

Process Parameters			Depth of Penetration Values		Percentage of Error
Wire Dias (mm)	Wire feed rate (mm/min)	Welding current (amp)	Experimental (mm)	Computational (mm)	
0.8	5600	271	2.50	2.5332	1.0400
0.8	5600	278	2.50	2.5126	0.9933
0.8	5600	286	2.50	2.5189	1.2150
0.8	5600	294	3.00	2.9813	1.2550
0.8	5600	302	3.00	2.9887	1.1750
0.8	5600	309	3.00	2.9912	0.4360
0.8	5600	317	3.00	3.0412	0.8280
0.8	5600	325	3.50	3.4896	0.9000
0.8	5600	332	3.50	3.4537	0.9320
0.8	5600	340	3.00	3.4695	0.9880

Table: A4.11 Depth of Penetration

Process Parameters			Depth of Penetration Values		Percentage of Error
Wire Dias (mm)	Wire feed rate (mm/min)	Welding current (amp)	Experimental (mm)	Computational (mm)	
1.0	4600	194	2.00	2.0167	0.8350
1.0	4600	202	2.00	2.0249	1.2450
1.0	4600	209	2.50	2.4876	0.4960
1.0	4600	217	2.50	2.4917	0.3320
1.0	4600	225	3.00	2.8873	3.7567
1.0	4600	232	3.00	2.9185	2.7167
1.0	4600	240	3.00	2.9367	2.1100
1.0	4600	248	3.50	3.4873	0.3629
1.0	4600	255	3.50	3.4913	0.2486
1.0	4600	263	3.50	3.4987	0.0371

Table: A4.12 Depth of Penetration

Process Parameters			Depth of Penetration Values		Percentage of Error
Wire Dias (mm)	Wire feed rate (mm/min)	Welding current (amp)	Experimental (mm)	Computational (mm)	
1.0	5600	271	2.50	2.5378	1.5120
1.0	5600	278	2.50	2.5286	1.1440
1.0	5600	286	3.50	3.4827	0.4943
1.0	5600	294	3.00	2.9138	2.8733
1.0	5600	302	3.00	2.9562	1.4600
1.0	5600	309	3.00	2.9593	1.3567
1.0	5600	317	3.50	3.4897	0.2943
1.0	5600	325	2.50	2.5134	0.5360
1.0	5600	332	3.00	3.0183	0.6100
1.0	5600	340	3.00	3.0127	0.4233

Table: A4.13 Depth of Heat Affected Zone

Process Parameters			Depth of HAZ Values		Percentage of Error
Wire Dias (mm)	Wire feed rate (mm/min)	Welding current (amp)	Experimental (mm)	Computational (mm)	
0.8	4600	194	1.50	1.5251	1.6733
0.8	4600	202	1.50	1.5328	2.1867
0.8	4600	209	1.50	1.5386	2.5733
0.8	4600	217	1.50	1.5397	2.6467
0.8	4600	225	2.00	1.9835	0.8250
0.8	4600	232	2.50	2.0375	18.5000
0.8	4600	240	2.00	2.0247	1.2350
0.8	4600	248	2.00	2.0364	1.8200
0.8	4600	255	2.00	2.0428	2.1400
0.8	4600	263	2.00	2.0482	2.4100

Table: A4.14 Depth of Heat Affected Zone

Process Parameters			Depth of HAZ Values		Percentage of Error
Wire Dias (mm)	Wire feed rate (mm/min)	Welding current (amp)	Experimental (mm)	Computational (mm)	
0.8	5600	271	2.00	2.0351	1.7550
0.8	5600	278	2.00	2.0384	1.9200
0.8	5600	286	2.50	2.5297	1.1880
0.8	5600	294	2.50	2.5327	1.3080
0.8	5600	302	2.00	2.0348	1.7400
0.8	5600	309	3.00	2.9832	0.5600
0.8	5600	317	3.00	2.9827	0.5767
0.8	5600	325	3.00	2.9845	0.5167
0.8	5600	332	3.00	3.0556	1.8533
0.8	5600	340	3.00	3.0823	2.7433

Table: A4.15 Depth of Heat Affected Zone

Process Parameters			Depth of HAZ Values		Percentage of Error
Wire Dias (mm)	Wire feed rate (mm/min)	Welding current (amp)	Experimental (mm)	Computational (mm)	
1.0	4600	194	1.50	1.5298	1.9867
1.0	4600	202	1.50	1.5486	3.2400
1.0	4600	209	2.00	1.9785	1.0750
1.0	4600	217	2.00	1.9637	1.8150
1.0	4600	225	2.00	1.9465	2.6750
1.0	4600	232	2.50	2.5425	1.7000
1.0	4600	240	2.00	2.0521	2.6050
1.0	4600	248	2.50	2.5607	2.4280
1.0	4600	255	2.50	2.5354	1.4160
1.0	4600	263	2.50	2.4598	1.6080

Table: A4.16 Depth of Heat Affected Zone

Process Parameters			Depth of HAZ Values		Percentage of Error
Wire Dias (mm)	Wire feed rate (mm/min)	Welding current (amp)	Experimental (mm)	Computational (mm)	
1.0	5600	271	3.00	2.9638	1.2067
1.0	5600	278	3.00	2.9752	0.8267
1.0	5600	286	2.50	2.5345	1.3800
1.0	5600	294	3.00	2.9348	2.1733
1.0	5600	302	2.50	2.4936	0.2560
1.0	5600	309	2.50	2.5136	0.5440
1.0	5600	317	3.50	3.5315	0.9000
1.0	5600	325	3.50	3.4883	0.3343
1.0	5600	332	3.50	3.4927	0.2085
1.0	5600	340	2.50	2.6127	4.5080

Table: A4.17 Hardness

Process Parameters			Hardness Values		Percentage of Error
Wire Dias (mm)	Wire feed rate (mm/min)	Welding current (amp)	Experimental	Computational	
0.8	4600	194	20.00	20.9130	4.5650
0.8	4600	202	20.00	20.7557	3.7785
0.8	4600	209	25.00	24.7171	1.1316
0.8	4600	217	20.00	20.0124	0.0620
0.8	4600	225	25.00	25.2629	1.0516
0.8	4600	232	15.00	15.5724	3.8160
0.8	4600	240	20.00	19.7470	1.2650
0.8	4600	248	20.00	19.8871	0.5645
0.8	4600	255	15.00	15.1108	0.7387
0.8	4600	263	20.00	19.2022	3.9890

Table: A4.18 Hardness

Process Parameters			Hardness Values		Percentage of Error
Wire Dias (mm)	Wire feed rate (mm/min)	Welding current (amp)	Experimental	Computational	
0.8	5600	271	20.00	19.9796	0.1020
0.8	5600	278	20.00	19.9672	0.1640
0.8	5600	286	20.00	19.2199	3.9005
0.8	5600	294	15.00	15.3415	2.2767
0.8	5600	302	20.00	19.4382	2.8090
0.8	5600	309	10.00	10.6328	6.3280
0.8	5600	317	15.00	15.7019	4.6793
0.8	5600	325	15.00	15.7675	5.1167
0.8	5600	332	15.00	15.9533	6.3553
0.8	5600	340	10.00	10.0337	0.3370

Table: A4.19 Hardness

Process Parameters			Hardness Values		Percentage of Error
Wire Dias (mm)	Wire feed rate (mm/min)	Welding current (amp)	Experimental	Computational	
1.0	4600	194	20.00	20.9353	4.6765
1.0	4600	202	20.00	20.3198	1.5990
1.0	4600	209	20.00	20.7426	3.7130
1.0	4600	217	25.00	20.0397	0.1588
1.0	4600	225	20.00	20.2920	1.4600
1.0	4600	232	15.00	15.6029	4.0193
1.0	4600	240	20.00	19.7789	1.1055
1.0	4600	248	20.00	19.9204	0.3980
1.0	4600	255	20.00	19.1451	4.2745
1.0	4600	263	15.00	15.2374	1.5827

Table: A4.20 Hardness

Process Parameters			Hardness Values		Percentage of Error
Wire Dias (mm)	Wire feed rate (mm/min)	Welding current (amp)	Experimental	Computational	
1.0	5600	271	15.00	15.8096	5.3973
1.0	5600	278	10.00	10.0992	0.9920
1.0	5600	286	20.00	19.2533	3.7335
1.0	5600	294	15.00	15.3761	2.5073
1.0	5600	302	20.00	19.4737	2.6315
1.0	5600	309	20.00	19.6690	1.6550
1.0	5600	317	20.00	19.7385	1.3075
1.0	5600	325	15.00	15.8042	5.3613
1.0	5600	332	15.00	15.9898	6.5987
1.0	5600	340	10.00	10.0696	0.6960